AMERICAN UNIVERSITY OF BEIRUT

CONTROLLING CYANOBACTERIAL BLOOMS BY ULTRASONIC IRRADIATION – LESSONS LEARNED FROM A REAL-WORLD APPLICATION IN A HYPEREUTROPHIC RESERVOIR

by
DANIA BAHIJ HAMZEH

A thesis
submitted in partial fulfilment of the requirements
for the degree of Master of Environmental Engineering (MEN)
to the Department of Civil and Environmental Engineering
of the Maroun Semaan Faculty of Engineering and Architecture at the American University of Beirut

Beirut, Lebanon
July 2020

AMERICAN UNIVERSITY OF BEIRUT

CONTROLLING CYANOBACTERIAL BLOOMS BY ULTRASONIC IRRADIATION – LESSONS LEARNED FROM A REAL-WORLD APPLICATION IN A HYPEREUTROPHIC RESERVOIR

by

DANIA BAHIJ HAMZEH

Approved by:

Dr. Ibrahim Alameddine, Assistant Professor
Department of Civil and Environmental Engineering
Advisor

Dr. Mutasem El Fadel, Chairperson and Professor
Department of Civil and Environmental Engineering
Member of Committee

Ghanem Oweis 14 Sept. 2020

Dr. Ghanem Oweis, Associate Professor
Department of Mechanical Engineering
Member of Committee

Date of thesis/dissertation defense: July 27, 2020

AMERICAN UNIVERSITY OF BEIRUT

THESIS, DISSERTATION, PROJECT RELEASE FORM

Student Name:

Hamzeh	Dania	Bahij
Last	First	Middle

● Master's Thesis ○ Master's Project ○ Doctoral Dissertation

☐ I authorize the American University of Beirut to: (a) reproduce hard or electronic copies of my thesis, dissertation, or project; (b) include such copies in the archives and digital repositories of the University; and (c) make freely available such copies to third parties for research or educational purposes.

■ I authorize the American University of Beirut, to: (a) reproduce hard or electronic copies of it; (b) include such copies in the archives and digital repositories of the University; and (c) make freely available such copies to third parties for research or educational purposes
after:

One ---- year from the date of submission of my thesis, dissertation, or project.
Two ✖ years from the date of submission of my thesis, dissertation, or project.
Three ---- years from the date of submission of my thesis, dissertation, or project.

DHamzeh 16-09-2020

Signature Date

This form is signed when submitting the thesis, dissertation, or project to the University Libraries

ACKNOWLEGMENTS

I would like to convey my sincere appreciation to my academic supervisor Dr. Ibrahim Alameddine for his continuous support throughout all stages of my research. His guidance and advice have expertly oriented my work.

In addition, I extend my gratitude to the rest of my committee, Dr. Mutasem Fadel and Dr. Ghanem Oweis for their assistance and helpful suggestions.

I would like to thank the University Research Board at the American University of Beirut for funding my research. I also express my gratitude to the Litani River Authority (LRA) management represented by Director General Dr. Sami Alawieh and Eng. Fadi Doumit for facilitating access to the lake, and to all the LRA Qaraoun team for their help and support throughout my sampling visits.

I am also grateful to my friends and family for their understanding and help, especially to my caring mother and supporting father.

Finally, the greatest credit goes to my husband Khalid. He has consistently encouraged me to achieve my goals.

AN ABSTRACT OF THE THESIS OF

Dania Bahij Hamzeh for Master of Engineering (ME)
Major: Environmental and Water Resources Engineering

Title: Controlling Cyanobacterial Blooms by Ultrasonic Irradiation – Lessons Learned from a Real-World Application in a Hypereutrophic Reservoir

Excessive nutrient loading and climatic changes have increased the frequency and intensity of harmful algal blooms (HABs) in freshwater systems globally. These blooms are responsible for the impairment of many water bodies. The use of ultrasonic treatment has been proposed as a novel environmentally friendly technology to control HABs. While results from laboratory-based experiments have shown promise, there has been little work conducted towards assessing the efficacy of the technology at the field-scale. In this study, we quantify and assess the efficiency of one of the largest field-deployed systems of ultrasonic transmitters (10 ultrasound emitting floating buoys) deployed in a large (220 Million m^3) hypereutrophic semi-arid reservoir. The collected ultrasonic recordings indicated that the transmitters were continuously emitting ultrasonic waves with dynamic frequencies, ranging between 27 and 47 kHz. An analysis of the propagation of waves in the water suggests that the ultrasonic influence of the system was largely confined to a radial distance of 30 m and to a depth of 5 m. Water quality data collected from the reservoir showed no statistically significant improvements in terms of chlorophyll-a, secchi disk depth, turbidity, and Microcystin-LR (MC-LR) levels in the treated areas as compared to a control site on the same lake. Moreover, water samples collected in close proximity to the ultrasonic buoys showed that algal concentrations tended to have a uniform distribution over the first 2 m below the water surface. Meanwhile, samples collected at the control site showed a typical drop in concentration with depth as a result of light limitation. Treated regions also tended to have a higher ratio of (MC-LR) toxin to chlorophyll-a in comparison to the control site. This suggests that the ultrasonic buoys impacted the buoyancy of the cyanobacteria and may have increased their environmental stress, leading to higher toxins levels. Our results provide a cautionary note to many water establishments that are currently planning to deploy commercially available ultrasonic buoys on their HAB-affected freshwater systems.

Keywords: ultrasound, cyanobacteria, eutrophication, chlorophyll, MC-LR, reservoir treatment

CONTENTS

LIST OF ILLUSTRATIONS

LIST OF TABLES

CHAPTER I

INTRODUCTION

Anthropogenic pollution has deteriorated the water quality and promoted the eutrophication of many freshwater systems globally (Rolle Longley et al. 2019, Wang et al. 2019). As eutrophication rates accelerated with increased nutrient loading and a warming climate, a sharp rise in the incidence of harmful algal blooms (HAB) has become evident (Gobler 2020, Huang et al. 2018, Su et al. 2017, Wolf et al. 2017). HABs are drawing the attention of water and environmental agencies all across the globe due to their adverse effects on human health, the environment, and the economy (Fang et al. 2019, Qin and Shen 2019). Among the many risks associated with HABs, one of the most alarming is their ability to release cyanotoxins during blooms (Moore et al. 2019, Weirich and Miller 2014). Elevated toxins levels in water have been linked to many skin diseases and to liver cancers (Fang et al. 2019, Sakai et al. 2007, Xiang et al. 2019).

Several mitigation measures have been proposed and adopted to control HAB across the globe. While reducing nutrient loads is key towards any restoration plan, such actions take time and some have not proven to be successful, especially in large and shallow lakes, such as lake Taihu in China (Qin et al. 2019). This is possibly due to the resuspension of nutrients from the lake sediments (Yu et al. 2016). Several physical, chemical and biological treatments have been proposed over the years to limit the scale and intensity of HABs events in the presence of elevated levels of nutrients. Algal skimming has been a commonly adopted low-cost mitigation measure. Nevertheless, concerns remain over the disposal/use of the collected biomass, with recent work criticizing skimming for shifting the problem from the water system to other environments (Eckersley and Berger 2018, Zeng et al. 2010, Zhong et al. 2012). The use of chemical algaecides, such as the application of copper-sulphate, hydrogen peroxide, luteolin and diquat, to restrict the growth and development of the cyanobacterial blooms is also a widely adopted and effective practice (Iwinski et al. 2017, Li et al. 2020, Zhou et al. 2020). Yet, several studies have highlighted the side-effects of using chemical algaecides, including the increase in the risks of toxin release to the environment as a result of algal cell lysis (Kinley et al. 2017, Tsai 2015, Zhang et al. 2019, Zhou et al. 2013) and potential impacts on non-target species (Jančula and Maršálek 2011). The modification of a system's food-web has also been proposed as a possible eutrophication mitigation; yet these methods have often been shown to negatively influence biodiversity and their success was marginal in oxygen-deficit media, typical of hypereutrophic systems (Sun et al. 2018).

The use of ultrasonic treatment has been proposed as an environmentally safe and novel HAB control method for freshwater systems (Rajasekhar et al. 2012a, Techer and Banas 2018, Tekile et al. 2017, Wu et al. 2019). The ability of ultrasound to damage microorganisms was first reported in the 1920s; yet the mechanism by which these organisms were damaged remained unclear. In the 1960s, acoustic cavitation caused by the ultrasound treatment was reported as the main inhibitive pathway (Greenly and Tester 2015, Kurokawa et al. 2016). Since then it became apparent that applying ultrasonic irradiations on cyanobacteria was able to inhibit their growth largely through rupturing their gas vacuoles and thus changing their buoyancy and limiting their photosynthetic capacity (Li et al. 2019). Gas vacuole collapse occurs due to the shear forces of the generated waves (Cameron et al. 2008). More recently, the collapse of cavitation bubbles was also shown to have a chemical impact (Joyce et al. 2003, Wu et al. 2012). High temperatures and pressures generated through ultrasonic treatment were found to produce free radicals from the water vapour that had a chemical inhibitive impact on the targeted cyanobacteria (Koda et al. 2009).

The effectiveness of ultrasonic treatment is a function of the adopted frequency and power (Dehghani 2016, Park et al. 2017a, Rajasekhar et al. 2012b). Several laboratory-based studies have focused on finding the optimal combination of frequency and power to control HABs (Table 1.1). In addition to the adopted ultrasonic frequency and power, the duration of sonication appears to play an important role towards the suppression of algal growth (Tan et al. 2018a). Longer exposure periods were shown to increase the rate of cyanobacterial colony degradation (Yamamoto and Shiah 2015). While sonication has proved to be successful at the laboratory scale, uncertainties remain regarding the basic core operational mechanisms. These uncertainties have made it difficult to determine its potential for upscaling (Tan et al. 2018b). Table 1.1 provides a summary of lab-scale studies conducted to assess the efficacy of ultrasonic treatment on the *Microcystis* cyanobacteria.

Table 1.1 Lab-scale studies assessing the efficacy of ultrasound treatment on Microcystis

Study	Volume (ml)	Frequencies (kHz)	Power (W/ml)	Time (sec)	Temperature (ºC)
(Kong et al. 2019)	500	120,430,740,1120	0.023-0.121	600	25 ± 3
(Duan et al. 2017)	500	35	0.043	5,30,60,300	25
(Liu et al. 2016)	400	20,40,60,80,120,150	0.1-1.5	120	-
(Fan et al. 2014)	50	580	2	300	20
(Zhang et al. 2006)	250	25	0.32	300	25 ±2
(Rodriguez-Molares et al. 2014)	600	21.5	0.014	600	22 ±1

Field-based assessment of the efficacy of the technology in large freshwater systems has been limited with inconclusive results (LaLiberte and Haber 2014, Lürling and Tolman 2014). The first field-scale ultrasonic transmitter to control cyanobacterial HABs was developed in Belgium in 1999 (Chen et al. 2020). Since then few experiments attempted to test the efficacy of ultrasonic treatment on inhibiting blooms at the pilot-scale and at the field-scale. A study conducted by Yu et al. (2013) subjected a pond dominated with *Microcystis aeruginosa* to ultrasonic irradiations of 28 kHz/900 W for 5 minutes. They reported that chlorophyll-a concentrations did not change significantly, with concentrations even increasing in some cases. In the shallow (average depth 1 m) lake of Senba in Japan (surface area = 0.32 Km^2), it was found that deploying 10 floating ultrasound emitting devices, each with an irradiation of 200 kHz/100 W, along with a water jet circulator module for two years was able to reduce the chlorophyll-a concentrations in the lake (Lee et al. 2002). A study conducted in a 400 m^2 enclosed section of Lake Taihu (China) assessed the efficacy of ultrasonic transducers fixed on a boat that emitted ultrasound waves with an irradiation of 20 kHz/800 W. The results showed that the ultrasonic system was able to lower the algae density in the targeted area of the lake (Lihong and Wei 2009). Ahn et al. (2007) reported the first successful field-scale application of ultrasonic treatment towards HAB control. Their ultrasonic device (22 kHz/630 W) combined with two water pumps was deployed on a 9,000 m^3 pond in South Korea for seven weeks. They reported the total algae and Chl-a concentrations decreased by around 50% and 40% respectively as compared to a nearby control pond (7,000 m^3). More recently, Schneider et al. (2015) reported that the deployment of four LG Sonic MPC buoys (similar to the one deployed in this study) for six months in Canoe Brook Reservoir Number 1 in New Jersey (volume = 2,860,000 m^3) was successful in controlling algal growth. Yet, their conclusions were based on comparisons with historical data as their study lacked a control site. On the other hand, several studies have reported no significant improvements in water quality following the deployment of ultrasonic devices. As study conducted in Golden Ham bay in the Netherlands found that Microcystis densities post–treatment remained similar to those in a neighbouring untreated location (Kardinaal et al. 2008). Another study in the Netherlands also reported a low efficiency of the ultrasound towards controlling cyanobacteria (Lurling et al. 2016). Additionally, Purcell et al. (2013b) reported that the mean Chl-a concentrations following the deployment of ultrasonic devices (40-50 kHz/ 40 W) in three drinking water reservoirs in the United Kingdom (volume ~ 900,000 m^3) were comparable to the levels measured in a nearby similarly sized reservoir.

In this study, we assess the efficiency of a full-scale implementation of an integrated ultrasonic treatment system deployed in a semi-arid hypereutrophic reservoir over the entire summer growing season. The efficiency of the treatment system was evaluated in terms of its ability to control HAB formations in the reservoir as well as alter MC-LR toxin release. We think that this work is the first long-term and large-scale scientific assessment that has examined systematically the efficacy of ultrasonic irradiation towards the inactivation of cyanobacteria in eutrophication-impaired water bodies, while assessing changes in MC-LR toxin release. Furthermore, we think that this work provides a timely opportunity to close the existing gap between the bench-scale assessments of the technology and its real-world application potential as an effective HAB control measure.

CHAPTER II

METHODOLOGY

2.1 Study area

The study was implemented on the Qaraoun Reservoir, Lebanon's largest freshwater body (Figure 2). It has a storage capacity of 220 million m^3. The lake volume fluctuates significantly by season and across years, due to changes in river inflow, precipitation, water use, and to a lesser extent evaporation and infiltration. The reservoir's surface area fluctuates between 4 and 11 km^2. Reservoir depths vary spatially, with the deepest section (near the dam) exceeding 45 m. The reservoir is a warm monomictic lake that stratifies between June and August, with temperature difference between the epilimnion and the hypolimnion exceeding 10˚C (Fadel et al. 2015). The reservoir is categorized as a hypertrophic aquatic system due to the excessive point and non-point pollutant loading that it receives from the Litani River (ELARD 2011, Jurdi et al. 2002, USAID 2005). As a result, the reservoir experiences consistent harmful cyanobacteria blooms throughout the growing season (late spring to early autumn). Although the lake had turned eutrophic in 1984, its water quality has significantly deteriorated post 2005 (Deutsch and Alameddine 2018). Starting in 2009, the reservoir has experienced toxic blooms of two cyanobacterial species (*Microcystis aeruginosa* and *Aphanizomenon ovalisporum*) (Fadel and Slim 2018). These blooms have been known to clog sprinkles and irrigation canals (canal 900) and negatively affect the touristic sector in the area. The Carlson trophic state index (CTSI) of the lake up until 2013 was less than 70 (eutrophic), post 2015 the CTSI exceeded 70 (hypereutrophic), pointing to the continuous deterioration of the lake's quality with time (Fadel et al. 2016). Chl-a concentrations in the reservoir have been regularly reported to exceed 5,000 µg/l during the growing season (Deutsch et al. 2018).

The Litany River Authority (LRA) is the governmental entity responsible for managing the entire Litani basin including Qaraoun reservoir. In an effort to control HAB in the lake, the LRA through the technical and financial support of the Dutch government have recently implemented a reservoir-scale algal bloom control and monitoring system that uses ultrasound treatment to suppress HAB events in the hypereutrophic reservoir. The system is composed of 10 solar-powered ultrasound emitting buoys (MPC-Buoys), refer to Figure 1, that were also instrumented with water quality sensors to provide a continuous overview on the water quality in the reservoir (LGSONIC 2020a). Each buoy was fitted with four ultrasound emitting transducers and three solar panels; the solar cells are monocrystalline and each panel has a size of 1,580 x 808 x 35 mm, providing 200 Wp rated power (Figure 1). The ultrasonic supplier claims that each buoy has a 250 m radius of influence and emits low-power ultrasound waves ranging between 5 and 10 W (LGSONIC 2020b). The frequencies that are emitted by the ultrasonic units are variable and tend to be tuned by LG Sonic on a regular basis based on the information they receive on the lake condition from the deployed in situ sensors as well as from remotely sensed data. Yet, the ultrasonic emitters have a maximum frequency of 50 kHz.

The majority of the 10 buoys were placed in the shallower northern part of the reservoir in the vicinity of the point of discharge of the Litani River (Figure 2). Only one device, buoy 37B, was placed in the middle section of the reservoir. No buoys were deployed in the deeper southern part of the reservoir, next to the dam. The objective of the system is to provide an opportunity to control the HABs, while minimizing the risks associated with algal toxin release.

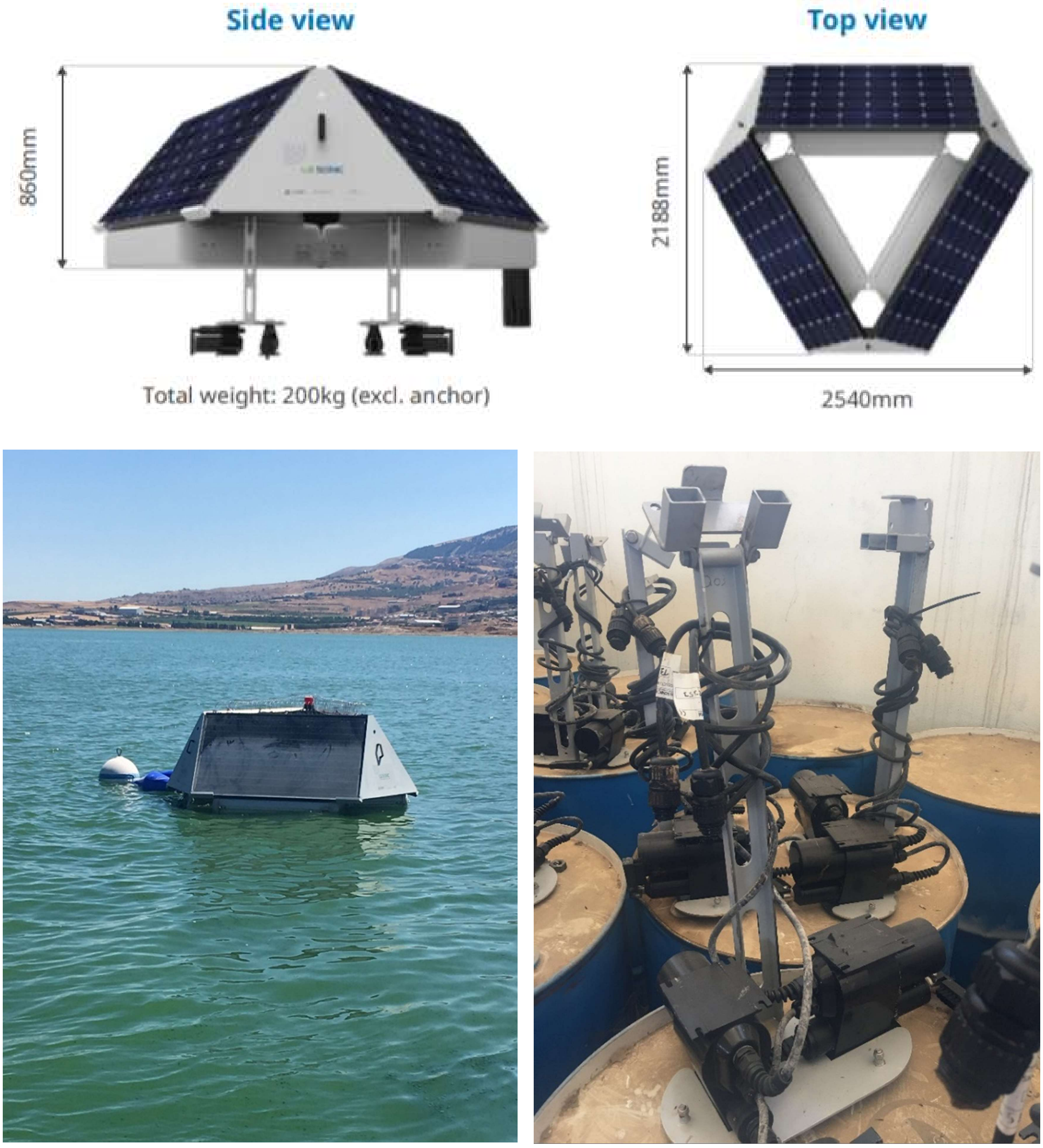

Figure 1 Side and top view of MPC buoys from LG Sonic webpage showing the dimensions of the device, a sample device deployed in lake Qaraoun and the transducers before being attached to the floating buoys

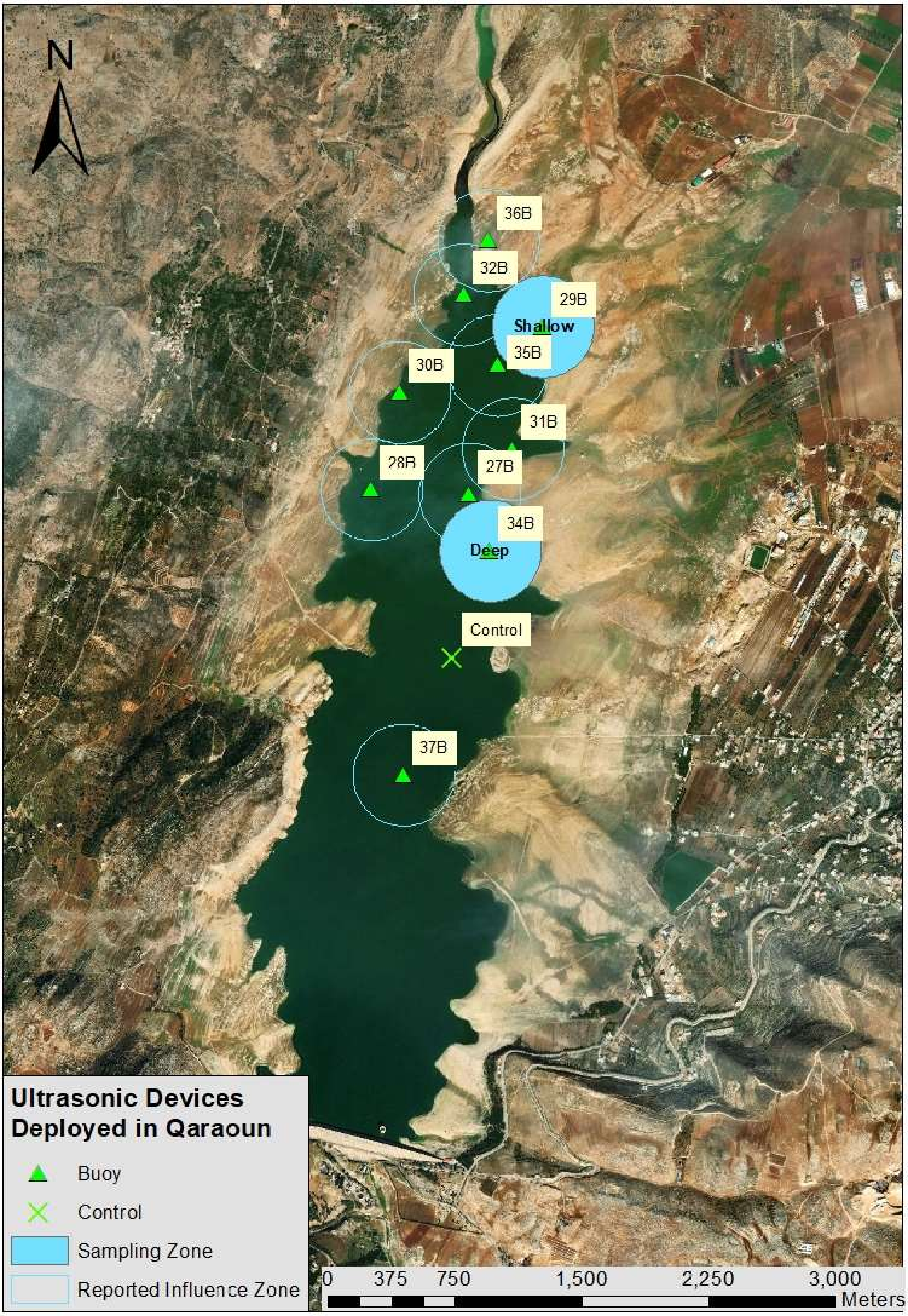

Figure 2 Buoy locations with reported area of influence, sampling locations and the control site

2.2 Sampling Plan

In an effort to assess the efficacy of the ultrasonic treatment, a sampling plan was developed to quantify the spatio-temporal variations of cyanobacterial and toxin levels at different locations influenced by the ultrasound treatment and to compare these levels with those measured concurrently at a control site within the same reservoir. This approach can block potential confounding effects such as changes in reservoir depth, surface temperature, thermocline strength, wind speed and direction, solar irradiation, dam release, and river flow. These factors are known to vary in space and/or time and are known to play an important role in modulating algae levels in the absence of ultrasonic treatments (Larson et al. 2016, Miller et al. 2013, Sinang et al. 2013).

Thirteen field-sampling campaigns were conducted between August and October 2019. During that period, algal blooms were regularly encountered. Blooms of *Microcystis* dominated up until mid-September, while *Aphanizomenon* blooms were observed in late September and early October. *Microcystis* dominated whenever water temperatures exceeded 25˚C (Fadel et al. 2015, Fadel and Slim 2018). On each sampling date, water quality samples were collected at station 29B (representative of the shallow regions of the lake), station 34B (representative of the deep regions of the lake), and at a control site that was located > 500 m away from any of the existing ultrasonic buoys (Figure 2). At each of the monitored locations, samples were collected at four radial distances away from the buoy, namely 5 m, 15 m, 30 m, and 60 m from the buoy. Additionally, water samples were collected at surface and over depth to assess potential changes in quality over the water column. Samples were thus taken at the surface (10 cm below surface), at 2 m, and at 5 m below the water surface.

Concurrently with the water quality sampling, the intensity and frequency of ultrasound were recorded at a depth of 10 cm, 2 m, 5 m and 7 m below surface water. Furthermore, continuous sound recordings were taken radially from the buoy up to a distance of 60 m away from the ultrasonic transmitters. Ultrasonic recordings at different radial distances and depths were conducted to determine the influence envelope produced by the ultrasonic buoys. In total, 23 water samples and 36 sound recordings were collected and analysed during each field visit. Table 2.1 summarizes the adopted monitoring plan with regards to the different locations and depths at which the water quality sampling and sound recordings were conducted.

Table 2.1 Summary of water samples and sound recordings locations and depths

Area	Distance from Buoy (m)	Depth (m)	Water Sample	Sound Recording
Shallow	5	0.1	√	√
		2	√	√
		5	√	√
		7		√
	15	0.1	√	√
		2		√
		5		√
		7		√
	30	0.1	√	√
		2	√	√
		5	√	√
		7		√
	60	0.1	√	√
		2	√	√
		5	√	√
		7		√
	Continuous from buoy up to 60 m	0.1		√
Deep	5	0.1	√	√
		2	√	√
		5	√	√
		7		√
	15	0.1	√	√
		2		√
		5		√
		7		√
	30	0.1	√	√
		2	√	√
		5	√	√
		7		√
	60	0.1	√	√
		2	√	√
		5	√	√
		7		√
	Continuous from buoy up to 60 m	0.1		√
Control	>500	0.1	√	√
		2	√	√
		5	√	√
		7		√

2.3 Water Quality Parameters

Water samples were collected via a horizontal Van Dorn water sampler. In addition, vertical profiles of temperature, total chlorophyll, and in vivo phycocyanin (by fluorometry) were recorded by deploying an EXO2-YSI Multiparameter 6-port water quality sonde at each location. Secchi disk depth (SDD), water temperature, pH, as well as the ratio of phycocyanin to total chlorophyll were recorded directly in the field. SDD was used to assess water clarity, using a 20 cm diameter black and white disk that was submerged in the water until it became invisible to the human eye. Low SDDs are a sign of eutrophic systems (Nishijima et al. 2018), which tend to have low transparency (Lee et al. 2015, Lei et al. 2020, Patel et al. 2020, Zou et al. 2020). Meanwhile, the EXO2 YSI sonde was used to collect complete vertical profiles of water temperature, pH, and the phycocyanin to total chlorophyll ratio. Collected water samples were also transported on ice to the laboratory for further chemical analysis; all analyses were completed within 48 hours of sample collection.

Chlorophyll-a concentrations were measured by filtering 50 mL samples through glass microfiber filter papers (Whatman 47 mm GF/C). The filter papers were then sonicated in 3 mL of boiled ethanol solution (90%). Extracts (filter papers together with ethanol) were seeped in 10 mL 90% ethanol solution overnight to be later clarified using centrifugation (15 mins at 3000-5000 G). Chlorophyll-a concentrations were determined based on absorbance (Standard Method 10200 (HS2)) (Rice et al. 2012) using a HACH DR 3900 spectrophotometer (Eaton and Franson 2005). The chlorophyll-a concentration was calculated as in Equation 1.

$$Chlorophyll\ a = \frac{29.62*(665a-665b)*Ve}{Vs*L} \qquad (1)$$

where: V_e: Volume of ethanol extract (mL)

V_s: Volume of water sample (L)

L: Path length of vial (cm)

665a: corrected 665a absorbance = 665-750

665b: corrected 665b absorbance after adding 0.01 ml of 1 mol/L HCl= 665-750

Algal cell diversity was also assessed by observing and counting algal species under an Upright Fluorescence microscope (Leica DFC 7000T). Since measuring algal biomass and diversity is a time consuming task (Sadeghian et al. 2018) and has been shown to correlate well with chlorophyll-a concentrations, the latter is more typically considered as the parameter of choice to assess the status of eutrophication (Binding et al. 2018). Meanwhile, the levels of total suspended solids (TSS) were determined by taking a known volume of the sample and filtering it through a pre-dried and pre-weighed glass fiber filter paper. The filter papers were then dried again in a 105^{o}C oven for at least an hour and re-weighed with the TSS residual. Under HAB events, TSS is mainly composed of alive and dead algae cells. Accordingly, Chl-a and TSS levels tend to have a strong positive correlation (Borkman and Smayda 2016).

Intracellular and extracellular MC-LR concentrations were determined using the Enzyme Linked Immunosorbent Assay (ELISA) technique (Lürling et al. 2014), which is a USEPA approved method (USEPA Method 546). The ELISA kits were procured from Eurofins Abraxis, INC (Part Number 520011OH). Collected water samples were divided into two sub-volumes. The first sub-volume was filtered through a GFC filter (Whatman, UK) and was immediately analysed; it represents the extracellular MC-LR levels. The second sample was exposed to three freeze/thaw cycles before filtration to lyse and to release the toxins from the cells. These represent the total MC-LR concentrations (i.e the intra and extra cellular toxins). In the absence of cell membrane damage, MC-LR is supposed to remain entrapped within the algal cells as intra-cellular MC-LR. Extra-cellular MC-LR is released to the water post algal cell lysing (Şengül et al. 2018).

Microcytin-LR concentrations were determined by fitting a semi-log curve of % Bo $\left(\frac{B}{Bo} \times 100\right)$ versus toxin concentrations, where B is the mean absorbance value for each standard, while B_0 is the mean absorbance value for the zero standard. A six standards ELISA kit ranging between 0.0 ppb and 5 ppb was used to calibrate the semi-log curve according to the procedure developed by Eurofins Abraxis, INC (Abraxis 2020). A preprogramed Excel-based optimization macros developed by Eurofins Abraxis, INC was used to estimate the MC-LR levels and to validate the results. Note that the samples that resulted in concentrations higher than the highest standard (5.0 ppb) were flagged and subsequently diluted with the sample diluent (provided with the Eurofins Abraxis Kit) before they were reanalysed. Most samples were either twice or four times diluted. Few extra-cellular concentrations were below the detection limit (0.006 µg/l) and were reported as 0.003 µg/l. Four total MC-LR concentrations were higher than the detection range even after dilution. These were reported as (> 350 µg/l).

2.4 Ultrasound Measurements

The frequency and intensity of the ultrasonic waves emitted by the buoys were recorded by deploying a factory calibrated AS-1 hydrophone from Aquarian Scientific. The AS-1 hydrophone has an omnidirectional response for a wide range of frequencies in the horizontal axis. It has a linear range between 1 Hz to 100 kHz ±2dB and a receiving sensitivity of -208 dB relative to 1V per 1µPa (40 µV/Pascal). The hydrophone has a passive piezo sensor that is connected to a pre-amplifier (PA4) that is operated by an external 9V DC power source. The PA4 is characterized by a high gain, wide dynamic range, and low noise. The signals from the PA4 were recorded on a Zoom H5 sound recorder. The recorder is capable of recording signals with a sampling rate of up to 96,000 Hz in a .wav format file (Hydrophones 2020, ZOOM 2020). Accordingly, sound frequencies up to 48 kHz can be captured by the adopted recording setup. Sound recordings were collected at the control site on each sampling date to account for natural differences in the sounds within the reservoir.

The analysis of the ultrasonic waves emitted from the buoys requires the determination of both their frequencies as well as their amplitudes. The sound frequency, which is the rate that sound pressure waves repeat themselves per second, is measured in Hertz (Hz) (EPA 1978, NPS 2018). While a typical human ear is sensitive to sounds with frequencies between 20 and 20,000 Hz, values beyond 20 kHz are not audible. Ultrasound is made of sound waves with frequencies above 20 kHz (Bilek and Turantaş 2013, Leighton 2007, O'Brien 2007). The hydrophone converted the sound wave pressure into electrical charges and stored them on a digital recorder in the form of audio samples after being augmented by an amplifier. The collected audio samples thus represent the energy of the sound waves (Christensson 2006, MicroPyramid 2017) and are thus proportional to Pascal (Betten et al. 2006, Pike 1998). The energy content held in a sound wave is measured in terms of its amplitude. A high amplitude implies a louder sound with higher energy carried in the audio pressure wave. Because averaging amplitudes of symmetrical waves, like the sine wave, results in a value of zero, the root-mean-square (RMS) method was used instead to estimate the amplitude of a wave. The RMS method squares the instantaneous amplitudes for every single unit of time, finds the arithmetic mean of the squared values, and then takes the square root of that average (Hansen 1995, Hass 2018).

The R software was used in this study to analyse the collected sound .wav files. The frequency spectrum for each file was first generated and plotted using the "*meanspec"* function from the *seewave* package (Sueur et al. 2008). This function converts the time basis sound wave to frequency basis plots by applying Fast Fourier Transformation (FFT) (DataQ 2020, rdrr 2019a). The RMS method is then implemeted to caclualte the amplitudes using the "*rms*" function from the same package (rdrr 2019b). Sound intensities are commonly reported in dB. As such, the amplitudes calculated by the RMS were converted to a ratio by dividing them with the lowest measured lake noise across all sampling trips. The obtained ratio was then log transformed to obtain the dB based sound amplitudes as shown in equation (2):

$$\text{Amplitude (dB)} = 10 * \log_{10} \frac{\text{Amp}_{\text{RMS}}}{\text{Amp}_{\text{ref}}} \tag{2}$$

where Amp_{ref} = 76.716 (least amplitude recorded at control site across all sampling trips)

2.5 Statistical analysis

The impact of the ultrasonic system on cyanobacteria and cyanotoxin levels was assessed by comparing the SDD, chlorophyll-a, TSS, and MC-LR concentrations measured next to the two ultrasonic units on a given day to their corresponding levels at the control station. Given that most environmental variables are log-normally distributed, it is typical to log transform (Ott 1995). Accordingly, all water quality variables were natural log-transformed based on the original data structure to meet the assumptions of parametric regression. A linear mixed-model was adopted instead of a conventional ANOVA to account for the repeated measurement experimental design (Kherad-pajouh and Renaud 2015). The mixed-model approach blocks the effect of the sampling date. The models were fit using the "*lme*" function from the *nlme* package (Pinheiro et al. 2020) in R (R Core Team 2019). The fitted linear mixed-effects model is based on the formulation of Laird and Ware (1982), but with nested random effects. The homogeneity of variance was assessed through the Levene Test under the *car* package (Fox and Weisberg 2011). Normality was assessed through the Shapiro-Wilk test prior to applying the mixed-model. In the event that the linear mixed-model showed statistical significance, the "*lsmeans*" function in R under the *lsmeans* package (Lenth 2016) was used to conduct pairwise multiple comparisons.

Statistical comparisons were conducted on the water quality parameters with regards to assessing differences along the radial distance from the ultrasonic transmitters (Figure 3) as well as over depth (Figure 4). The statistical assessment was also conducted to determine if the efficacy of the system varied between the deep (34B) and shallow (29B) buoys deployed in the lake. Similarly, the radial variations of sound amplitude were evaluated both in the deep and shallow areas and compared to readings collected at the control site. All statistical analysis were conducted in the R software (R Core Team 2019).

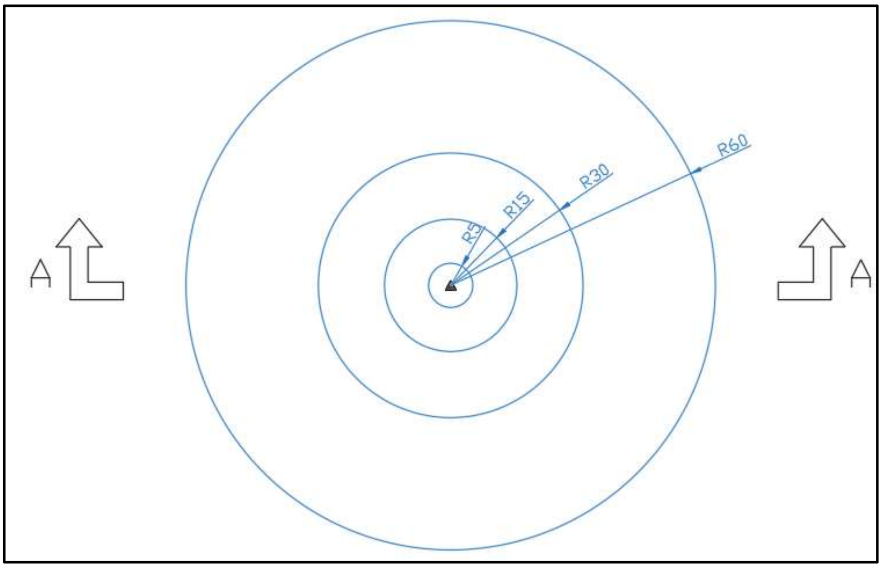

Figure 3 Radial locations of collected water samples and sound recordings

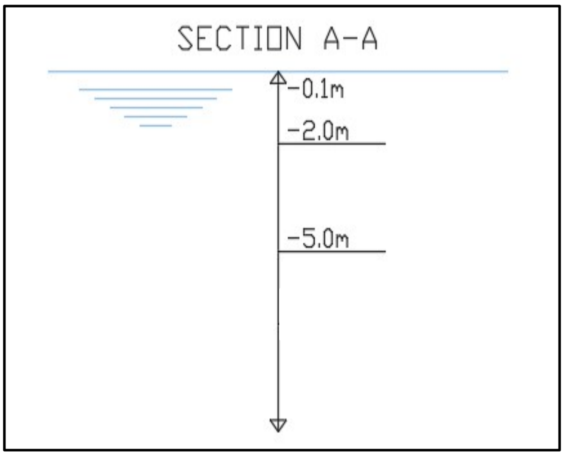

Figure 4 Vertical locations of collected water samples and sound recordings

CHAPTER III

RESULTS AND DISCUSSIONS

3.1 Reservoir's water quality

The physical conditions of the lake varied significantly over the sampling period that extended from mid-August to early October 2019. Figure 5 illustrates the vertical temperature profile of the lake down to a depth of 11 m. The surface temperature cooled by around 3 ℃ between August and early October. Prior to September 18th, a 3 ℃ difference existed between the surface and 11 m below. Following that date, the difference between the two depths did not exceed 1 ℃. Casting the sonde for depths exceeding 30 meters showed that the lake was stratified prior to the 18th of September (Figure 5). Following that date, the thermocline started to weaken and disappeared in the shallow sections of the lake; yet it persisted in the deeper parts. Changes in water temperature play a key role in modulating the intensity of algal blooms, the quantity of toxins they released, and algal diversity (Fang et al. 2018, Wells et al. 2020).

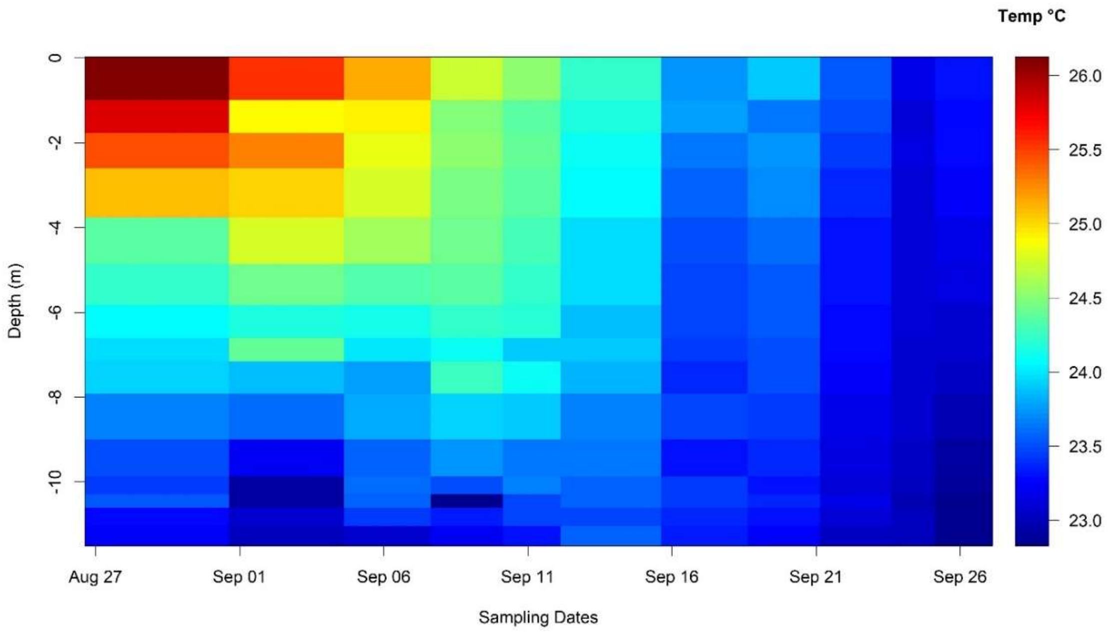

Figure 5 Lake averaged vertical profile of water temperature over the sampling period

Over the entire sampling period and irrespective of the meteorological conditions, the reservoir consistently experienced algal blooms. Prior to the 9th of September, *Microcystis aeruginosa* was the dominant cyanobacteria in the reservoir. Starting on September 11th, *Aphanizomenon ovalisporum* started to appear and to dominate the total cyanobacterial community (Figure 6). More than 75% of all SDD measurements were lower than 1.1 m (Figure 7). The highest SDD recorded was 1.4 m and it occurred on the 18th of September. Surface Chl-a levels ranged between 36.1 and 1,363 µg/l, while one measurement at 60 m away from buoy 29B (shallow area) exceeded 5,000 µg/l on the 23rd of September. Similar to the findings of Chawla et al. (2020), Chl-a had a strong negative correlation with SDD (Spearman correlation = -0.76, p-value $< 2.2*10^{-16}$) (Figure 8). Chl-a levels had a positive correlation with temperature (Spearman correlation = 0.38, p-value $< 2.02*10^{-9}$) and pH (Spearman correlation = 0.30, p-value $< 3.68*10^{-6}$). The correlation with pH is probably due to the high consumption of CO_2 from surface water by the algae (Rarrek et al. 2018, Singh

2019), while the correlation with surface temperature is typical of cyanobacteria blooms (González and Puntarulo 2020, Rijal Leblad et al. 2020). As expected, the Chl-a concentrations decreased smoothly with depth. Only on September 3rd and October 1st, the median concentrations at a 2 m depth were slightly higher than those measured at the surface; yet these differences were not statistically significant at the 95% confidence level. Figure 7 traces the development of Chl-a concentrations over time at the surface and at 2 m and 5 m below the surface. TSS levels largely mirrored those of Chl-a (Spearman correlation = 0.76, p-value $< 2.2*10^{-16}$) (Figure 8). TSS concentrations ranged between 5 and 30 μg/l. Overall, TSS, like Chl-a, showed a smooth consistent drop with depth with only a few exceptions.

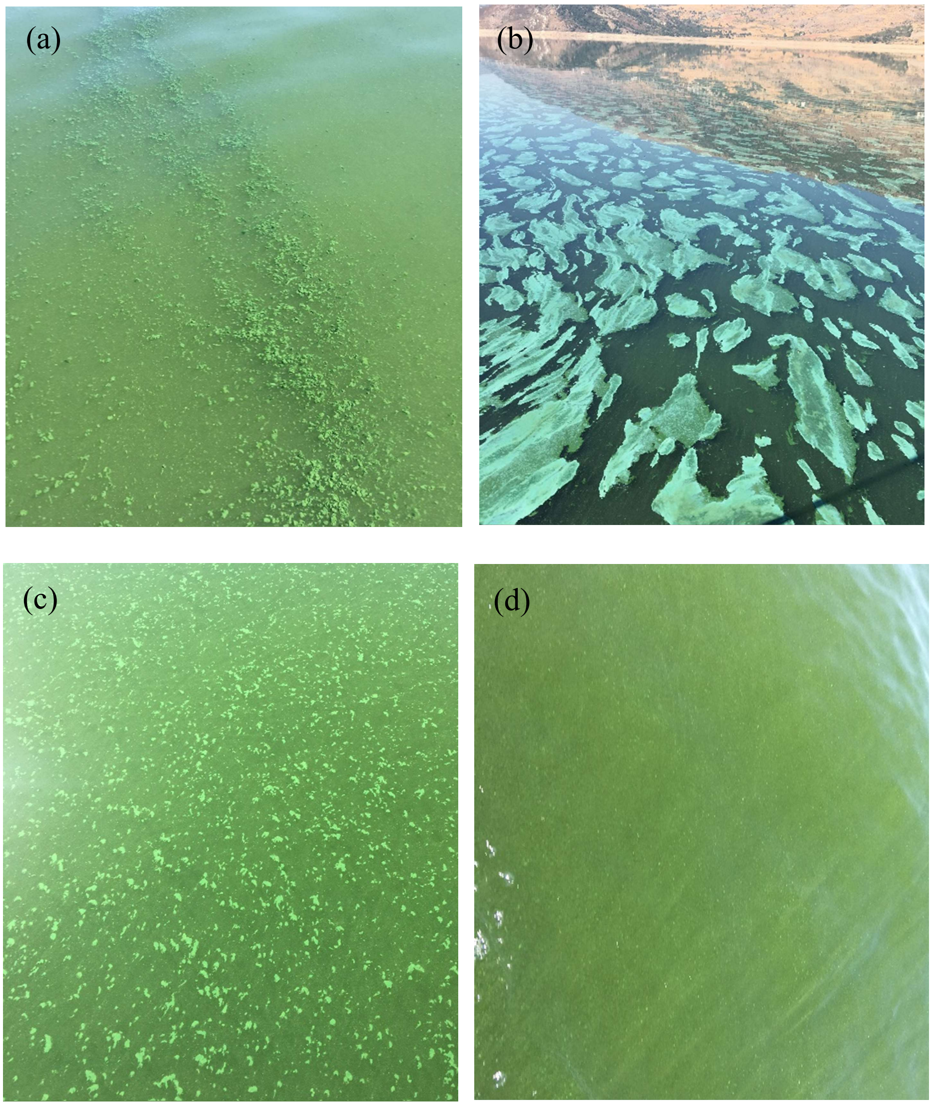

Figure 6 Cyanobacterial blooms observed in the reservoir. (a) September 6th: stable lake conditions with low winds and dominance of granular-like green cyanobacterial colonies; (b) September 11th: stable lake conditions with low winds and dominance of mats of blue-green colonies; (c) September 26th calm lake conditions with low winds and scattered green colonies; (d) October 1st: windy conditions with waves, algae appear dispersed and not clumped

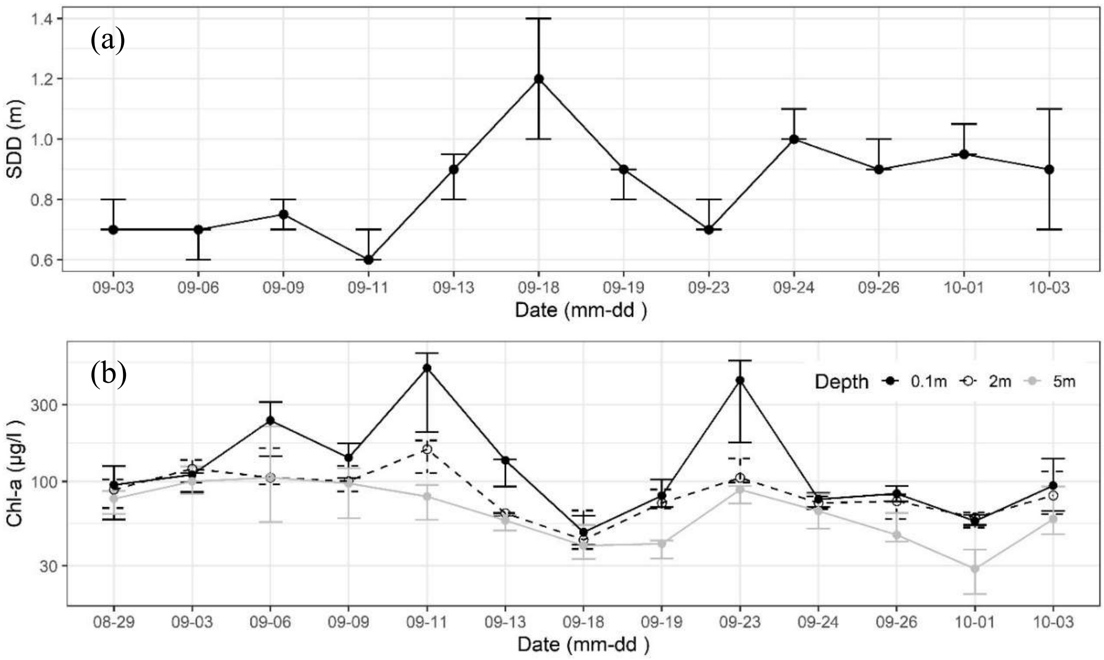

Figure 7 Temporal changes in (a) Secchi disk depth (SDD) and (b) chlorophyll-a levels. The circle represents the median level measured on a given day across the lake, while the vertical segments represent the first and third quartiles

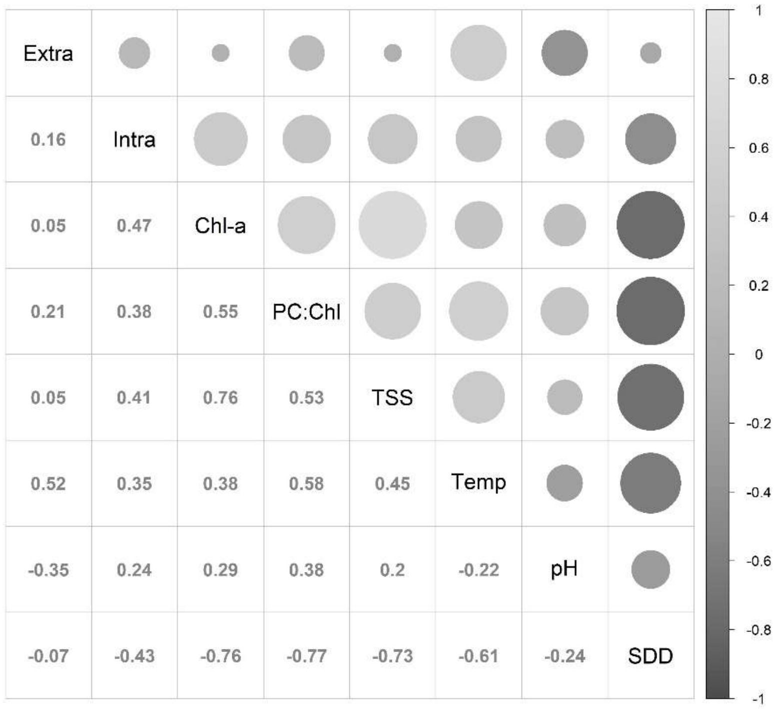

Figure 8 Correlations between the measured water quality parameters

The PC:Chl ratio is a metric that has been used to predict cyanobacterial blooms (Yacobi et al. 2015, Yan et al. 2018). It tends to be high during bloom events (Gobler et al. 2013). As can be seen in Figure 9, the ratio was consistently above 0.7 prior to September 18 indicating that cyanobacteria constituted a high proportion of the measured total phytoplankton community. It also appears from the PC:Chl ratio that the cyanobacterial community peaked in dominance towards September 6. Post September 18th, the PC:Chl ratio dropped below 0.6. The ratio appears to decrease rapidly with depth and reaches zero between 5 and 8 m across all dates. This highlights the strong light limitation that the algae experiences in the reservoir during blooms. Moreover, the ratio appears to show a strong correlation with temperature (Spearman correlation = 0.58, p-value < $2.2*10^{-16}$) and pH (Spearman correlation = 0.38, p-value < $1.08*10^{-9}$) (Figure 8).

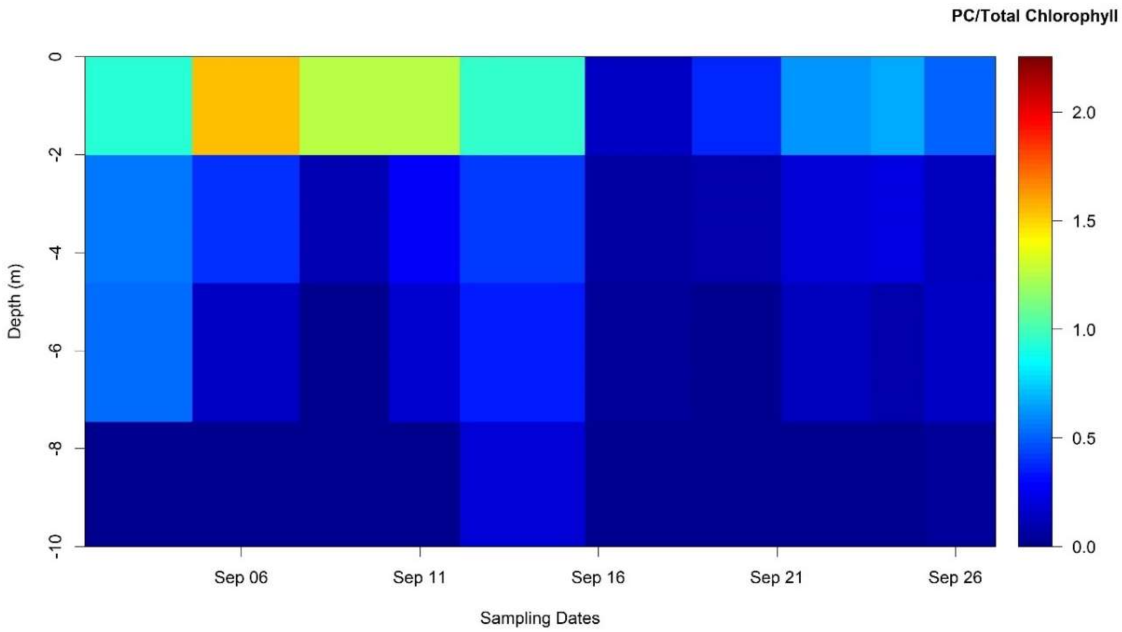

Figure 9 Vertical profile of the PC:Total chlorophyll ratio over the sampling period at the control site

Across all sampling dates, the extra-cellular MC-LR concentrations both at the surface and at a depth of 5 m were below the 1 µg/l provisional WHO guideline (WHO

2003) (Figure 10). Yet, several intra-cellular concentrations (Figure 10) exceeded the 1 μg/l limit, especially for surface samples. More than 45% of the total MC-LR levels exceeded the WHO set guideline. The median concentrations of extra-cellular MC-LR at the surface and at a depth of 5 m were relatively similar, except for the period stretching between September 9 and 13. This pattern mirrors the vertical variability observed in Chl-a concentrations between surface and 5m deep during that period (Figure 7). Intracellular MC-LR concentrations at the surface were consistently higher than those at 5m deep, except on the first two sampling dates. Similar to the findings of Rinta-Kanto et al. (2009), the intracellular MC-LR levels were highly correlated (Figure 8) to the measured Chl-a concentrations (Spearman correlation = 0.47, p-value = $3.36*10^{-10}$).

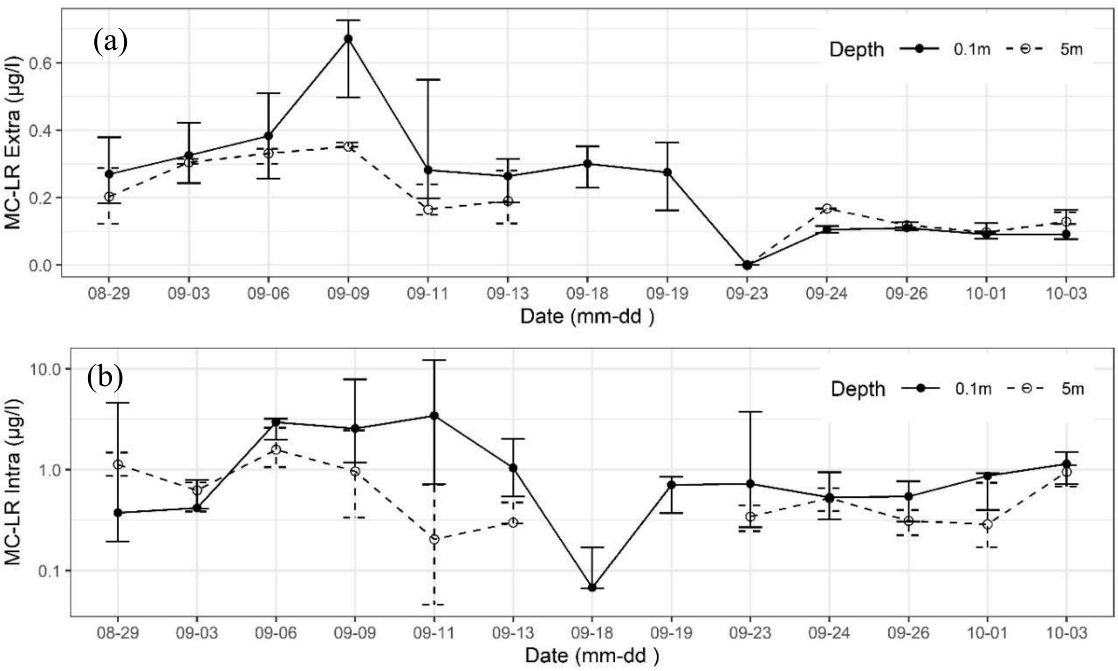

Figure 10 Temporal variability of (a) extra-cellular MC-LR and (b) intra-cellular MC-LR concentration (μg/l). The circle represents the median level measured on a given day across the lake, while the vertical segments represent the first and third quartiles.

3.2 Ultrasound measurements in the reservoir

3.2.1 Ultrasonic sound waves

Given that the effectiveness of the ultrasonic treatment depends on the frequency emitted, period of exposure, as well as the intensity (power) of the ultrasound wave, we analysed the recorded sound files at different locations over all sampling dates. Sound levels along the radial distance from the ultrasonic transmitters dampened continuously and became unidentifiable after 30 m. Figure 11 presents a sample of the sound level recordings that show the fast decay of the sound levels with radial distance away from the ultrasonic device. Note that the same pattern was observed for both buoys (deep and shallow areas) and during all sampling dates except on September 13, when it appeared that the ultrasonic device in the deep area (34B device) was not operational during the time of sampling. Park et al. (2019) have also reported a rapid drop in sound pressure away from the ultrasound source (36 kHz/300 W) along the Geum River, South Korea. They estimated that the sound pressure decreased by ~80% in the first meter.

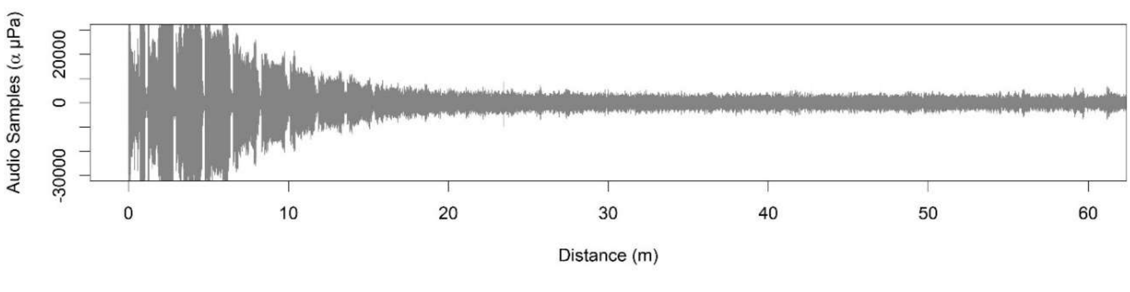

Figure 11 Surface sound wave recordings on September 6 (buoy 29B)

Prior to September 23, all sound recordings, regardless of their radial distance tended to have a clear repetitive pattern that regularly recurred in time. The ultrasonic waves recorded at different water depths showed that the repetitive pattern was apparent in all surface and 2 m depth recordings. At 5m, these patterns became more difficult to detect, while recordings at 7 m showed no clear pattern as natural lake noises dominated. Figure 12 shows how the ultrasonic pattern deteriorated with depth. The period of the repeating pattern ranged between 3.8 and 4.9 seconds. Figure 13 shows a sample of the repetitive pattern that was measured near Buoy 29B on September 6. The period on that date was determined to be 4.25s. Post September 23, no clear recurring pattern could be observed across all sampling locations over the 20 second recordings (Figure 13). The observed change in the audio recordings between the two dates may indicate a possible change in the emission settings of the ultrasonic devices in response to changes in water quality. Note that throughout the field sampling campaign, the ultrasound units were emitting continuously with the exception of device 34B that was off on September 13. The continuous operation of the ultrasonic devices at low sound pressures has been reported to be the most cost effective practice for field applications (Park et al. 2017b).

Given that the ultrasonic emitting devices use low power (5 to 10 W) (LGSONIC 2020a), the average power per unit volume of water in a hemi-sphere with a 1 m radius from the centre of the buoy was calculated and found to be 4.77×10^{-6} W/ml. Power per unit water volume is expected to decrease even further with increased radial distances. These values are significantly lower than any of the reported field-based (Lee et al. 2002, Lihong and Wei 2009, Ahn et al. 2007, Yu et al. 2013) or laboratory-based power values (Table 1.1).

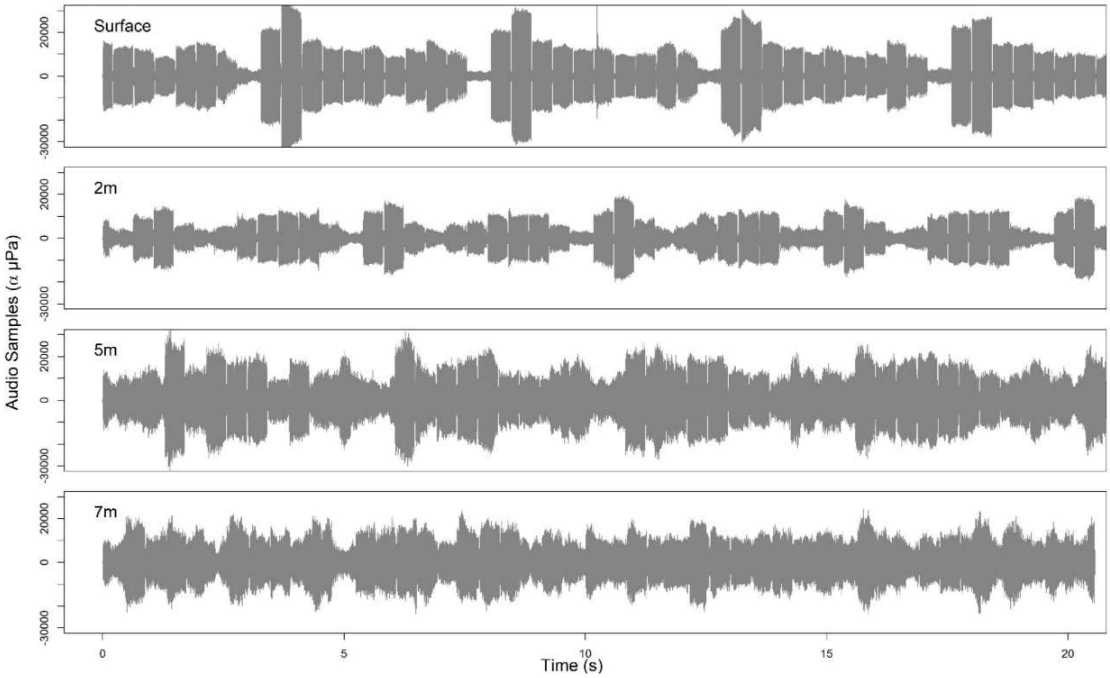

Figure 12 Changes in recorded sound waves by depth (September 6th next to Buoy 29B)

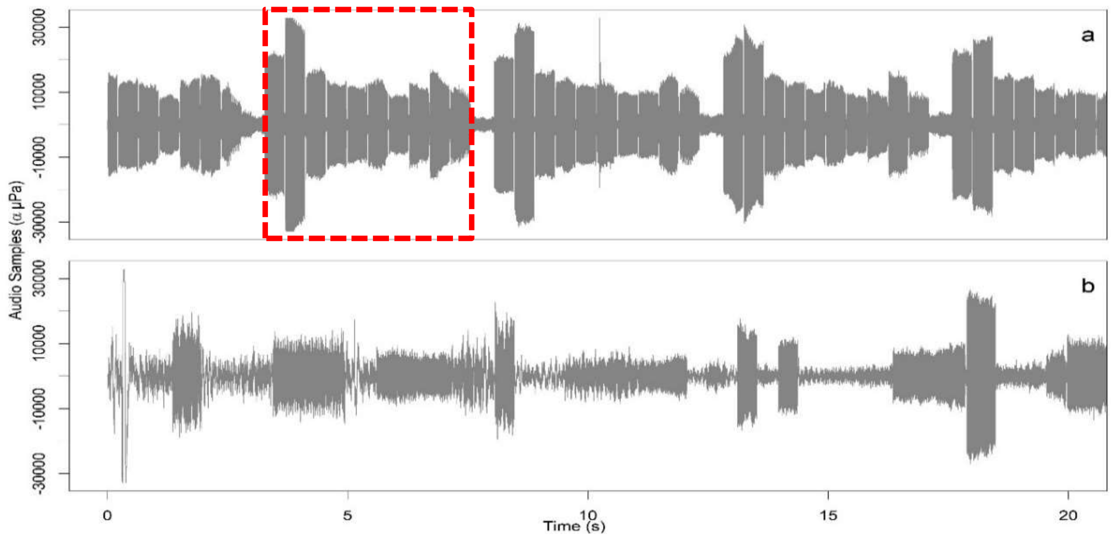

Figure 13 Surface Recording next to Buoy 29B on (a) September 6th and (b) September 24th

3.2.2 Ultrasonic frequencies and amplitudes

Frequency spectrums were generated to determine the frequencies of emitted sound waves. The summary of the highest harmonic frequencies revealed that most emissions occurred between 27 and 47 kHz, regardless of the site and sampling date.

This indicates that the ultrasonic units were not emitting one frequency but instead a set of frequencies (27, 28, 30, 31, 33, 34, 35, 36, 37, 38, 42, 44 and 46 kHz) in all recorded spectrums (Figure 14 a). Three additional frequencies (29, 43 and 47 kHz) were also observed starting on September 23rd (Figure 14 b). This provides further evidence of a possible modification in the emission program of the ultrasound devices. Prior to September 23, the frequencies 37 and 44 kHz had the highest energy content next to buoy 34B (deep section). Post September 23, frequencies between 30 and 34 kHz had the highest energy. On the other hand, the highest harmonic frequencies at the shallow buoy (buoy 29B) ranged between 27 and 34 kHz during all sampling dates, indicating that the two ultrasonic devices operated independently and did not necessarily function with similar settings.

Overall, the recorded frequencies were consistent with what has been recommended for field-scale ultrasonic treatment systems (20 to 50 kHz), as emissions in these frequencies are both economical and safer than emitting higher ultrasonic frequencies (Li et al. 2014, Park et al. 2017b). Analysing the sound spectrum at the control site showed similar frequencies to those near the operating buoys but with significantly lower amplitudes. This is expected since the ultrasound waves reaching the control sites would have lost their intensity as they travel away from the transmitters.

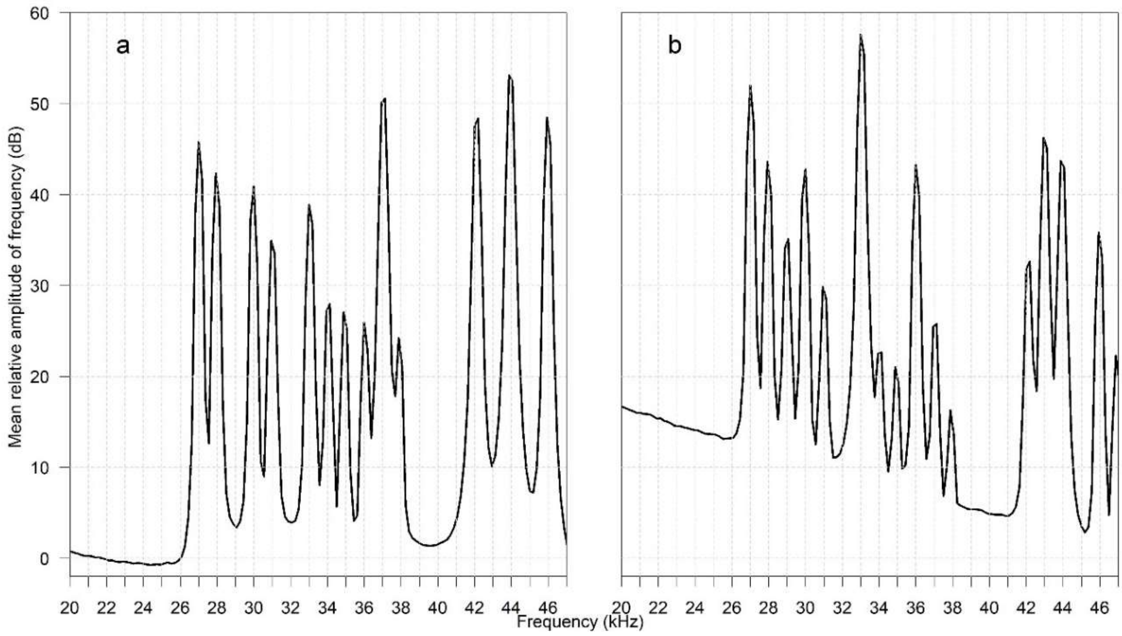

Figure 14 Mean relative amplitude of the frequencies recorded at 10 cm below water surface (a) next to buoy 34B on September 9 and (b) next to buoy 29B on October 3

3.2.3 Efficiency of the ultrasound along radial distances

The mixed-model results indicated that there were no statistically significant difference between the SDD, TSS, and Chl-a levels measured at the control site on one hand and all sampling locations in close proximity to the ultrasonic buoys (5 m, 15 m, 30 m and 60 m away from the buoys). As shown in Figure 15, the medians of the Chl-a concentrations normalized by the concentrations at the control did not significantly vary between the different radial distances across all depths. Yet, it appears that the surface Chl-a levels tended to be slightly lower than the control across all radial distances. This was consistent for both the shallow and deep buoys. These reductions were no longer apparent for samples collected at a depth of 2 and 5 m. The only statistically significant difference in water quality was a marginal drop in the median TSS level measured 60 m away from buoy 29B and at a depth of 2 m as compared to the median concentration measured at the same depth at the control site. The results clearly indicate that the ultrasonic devices were not successful in supressing cyanobacterial growth or their proliferation within their supposed areas of influence. Interestingly, the water quality improvements that were observed at a distance of 5 m from the buoys were only marginal and not statistically significant. This suggests that the emitted ultrasonic waves were unable to collapse the gas vacuoles of the *Microcystis* cells. These results concur with the findings of Park et al. (2019), who reported a marginal reduction (drop of 15%) in Chl-a levels within 1 m away from their deployed ultrasonic device after sonicating for 5 minutes in a small 4 m^3 pond. Yet, our results disagree with the findings of Inman (2004), who reported that deploying an ultrasonic emitter operating at 28 kHz and with a low power intensity (40 W) resulted in a marginal, yet statistically significant drop in chlorophyll-a concentrations in a small pond with an area of 300 m^2. It should be stressed though that the scale of our studied system (area = 12 Km^2; volume = 220 MMC) is several orders of magnitude larger than the systems assessed in both of these studies.

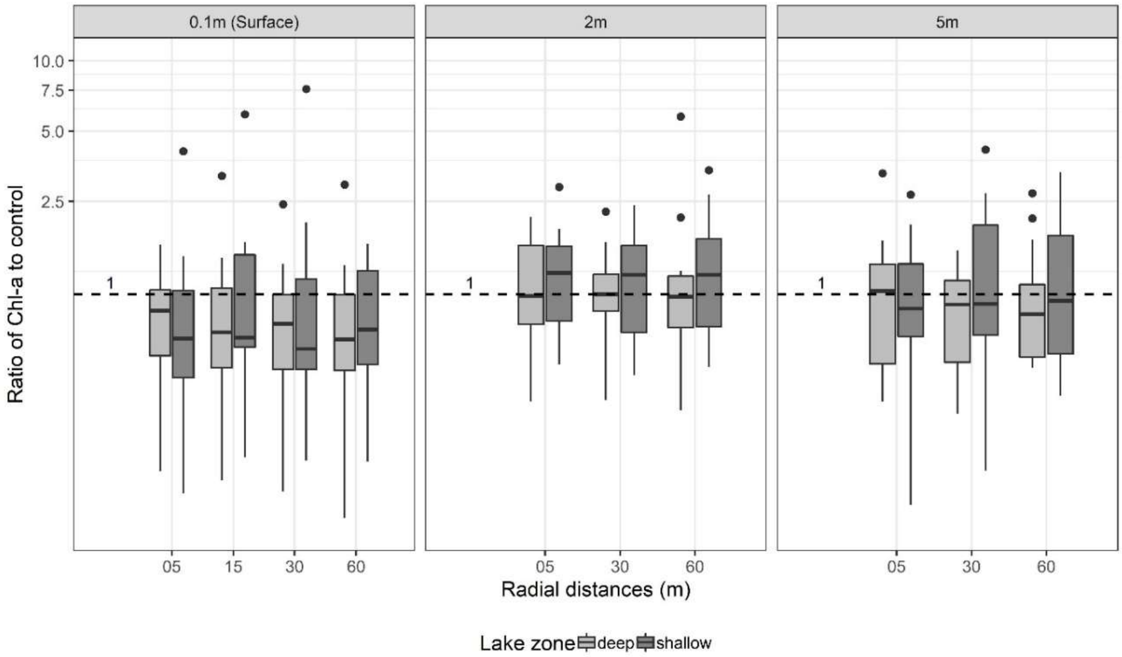

Figure 15 Boxplots of Chl-a concentration ratios to control over radial distances at surface, 2m and 5m deep

Concerning the MC-LR levels at the surface and at a depth of 5 m, the mixed-model analysis showed that there were no statistically significant differences in the extra and intra-cellular MC-LR concentrations measured in the regions that were irradiated with the ultrasound as compared to those at the control site. Median toxin concentrations at 5, 15, 30, and 60 meters away from the ultrasonic devices were largely similar in magnitude. This indicates that the ultrasonic waves did not result in a significant rupture of the cells, as that would have led to increased extracellular MC-LR levels and a drop in the intracellular levels. This is supported by the findings of Lee et al. (2001), who reported that low frequency ultrasonic irradiation (28 kHz), like the one used in Qaraoun Reservoir, are unable to cause cell rupture that leads in turn to toxin release. While several studies (Ma et al. 2005, Song et al. 2006, Song et al. 2005) have reported that the emitted ultrasounds are able to degrade extracellular MC-LR; our results show that this degradation process was ineffective. Measured extracellular MC-LR levels in the vicinity of the ultrasound emitting devices were not lower than those measured at the control site. This could be due to the low frequencies used in the deployed devices. Note that previous work has reported that marginal toxin degradation is expected with the use of low ultrasound frequencies; frequencies as high as 640 kHz were found to be needed to degrade at least 50% of the extracellular toxin under laboratory conditions (Song et al. 2006, Song et al. 2005).

The ineffectiveness of the deployed low frequency ultrasound treatment system to control HABs concurs with several laboratory-based studies that have concluded that higher ultrasonic frequencies are needed (Peng et al. 2020, Yamamoto et al. 2015). Joyce et al. (2010) reported that the optimal frequency needed to control *Microcystis aeruginosa* was 580 kHz. Their results showed that emitting at 40 kHz was only able to declump the *Microcystis* colonies. Wu et al. (2012) reported that opting for a frequency as low as 20 kHz can be effective only if it is accompanied with the use of high intensity (0.0403 W/ml), which appears to be impractical to secure in solar powered units like the ones we assessed where the power within the first 1 m drops to 4.77×10^{-6} W/ml. Hao et al. (2004b) also reported that high frequency ultrasounds (frequencies as high as 1.7 MHz) were 50% more effective in controlling *Spirulina platensis* growth as compared to 20 kHz. The increased efficiencies of high ultrasonic frequencies (>100 kHz) in controlling cyanobacteria is probably due to the fact that these frequencies are closer to the resonance frequencies of algal gas vacuoles; resonance promotes gas vesicles rupture and helps to inactivate cyanobacterial growth (Hao et al. 2004a, Li et al. 2019). It should be noted that several studies have concluded that the effectiveness of ultrasound treatment in controlling algal proliferation is species specific (Park et al.

2017b). Tang et al. (2004) reported that the effectiveness of the ultrasound appears to be more selective to cyanobacteria with gas vacuoles, like *Microcystis aeruginosa*. Yet, Jachlewski et al. (2013) later showed that cyanobacteria lacking gas vacuoles were equally susceptible to the effects of sonication, while Purcell et al. (2013a) found that ultrasound affected filamentous species more than uni-cellular and colonial cyanobacteria. In our study, we found no statistically significant differences in the effectiveness of the deployed ultrasounds with regards to the two cyanobacterial species encountered in the lake, namely *Microcystis aeruginosa* (colonial and with gas vacuoles) and *Aphanizomenon ovalisporum* (filamentous and without gas vacuoles).

Finally our assessment of the radial variations in the ultrasound amplitude showed that the rate at which the amplitudes degraded varied significantly as a function of water depth (Table 3.1). At surface, the recorded amplitudes experienced a sharp drop between 5 to 15 m (around 25% drop in the amplitude). Beyond 15 m, the drop was largely insignificant. These findings indicate that the ultrasonic irradiations had a short propagation range (Heng et al. 2009). At a depth of 2 m, the drop in the amplitude was more gradual and occurred across the entire 60 m radial distance. The measured amplitudes at a depth of 5 m showed a significant drop between 15 and 30 m. Amplitudes before 15 m were largely similar as were those after 30 m. The amplitudes at a depth of 7 m did not significantly vary with radial distances. At all depths, the amplitude at the control site was much lower than all those recorded within a 60 m radius of the ultrasonic buoys. Figure 16 shows the variability of median amplitudes normalized to the amplitude at the control site as a function of radial distances. The normalization of the amplitudes allows for cancelling out the impact of background lake noise. The audio amplitudes next to both devices follow similar decaying patterns, yet the initial intensity at surface in the shallow area seems higher than those recorded in deep areas. However, the amplitude attenuated faster next to buoy 29B and the intensity at 60 m maintained less of the initial value. Heng et al. (2009) stated that ultrasonic irradiations had short propagation ranges, which supports the rapid decrease in the observed amplitude.

Table 3.1 Statistical results of the amplitudes radial variation at different lake depths

Buoy	Water depth	Radial distances with statistically significant differences in amplitude
Deep Area (next to buoy 34B)	Surface	5m with all distances Control with all distances
	2m	5 with all distances 15 m with 60 m Control with all distances
	5m	5 m with distances except 15 m 15 m with 30 and 60 m Control with all distances
	7m	5m with 60 m 15m with 60 m Control with all distances
Shallow Area (next to buoy 29B)	Surface	5m with all distances Control with all distances
	2m	5 m with distances except 15 m 15 m with 60 m Control with all distances
	5m	5m with 60 m 15m with 60 m Control with all distances
	7m	15 m with 60 m Control with all distances

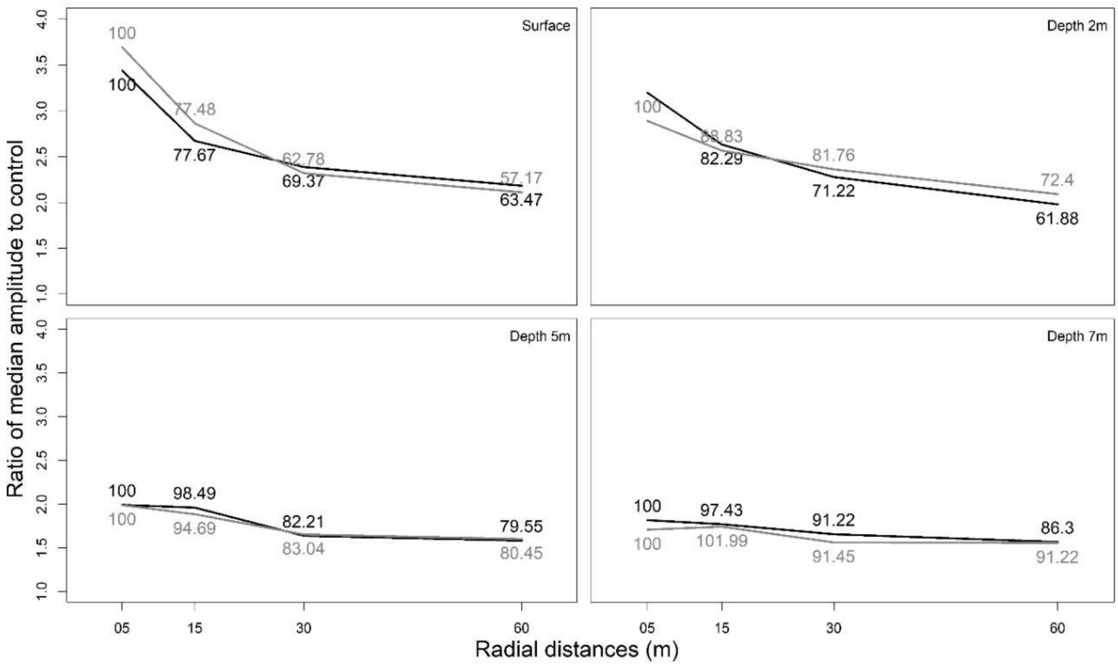

Figure 16 Ratio of median amplitude to control along radial distances at different depths grey for the shallow and black for the deep area

3.2.4 Efficiency of the ultrasound over depth

The results indicated that the changes in Chl-a levels over depth differed significantly between the control site on one hand and all sampling locations in the vicinity of the ultrasonic buoys on the other. At the control site, Chl-a concentrations consistently decreased with depth; surface concentrations were significantly higher than those measured at 2 m (p-value=0.0044) and at 5 m (p-value=0.0003) (Figure 17). This is to be expected given the strong light limitation during HAB events. Sampling locations in the vicinity of the ultrasonic units showed a different pattern; concentrations at the surface and at a depth of 2 m were found to be largely similar in magnitude and statistically higher than levels observed at a depth of 5 m. This pattern was consistently observed at 5 m, 30 m, and 60 m away from the ultrasonic buoys (Figure 17). This could possibly suggest that the ultrasound may have been able to alter the cyanobacterial buoyancy and push the cells deeper into the water column. This behaviour has been reported previously, whereby observed cyanobacterial cells tend to sink when exposed to ultrasonic waves (Kotopoulis et al. 2009, Li et al. 2014, Wu et al. 2011). Yet, our findings imply that while the ultrasonic devices may have been able to push some of the cyanobacterial cells down by at least 2 meters and promote their light limiting conditions, the fact that the lake was hypereutrophic probably resulted in new cyanobacterial cells readily replacing the ones submerged. This is supported by the fact that surface concentrations of Chl-a near the buoys were statistically similar to those measured at the control site.

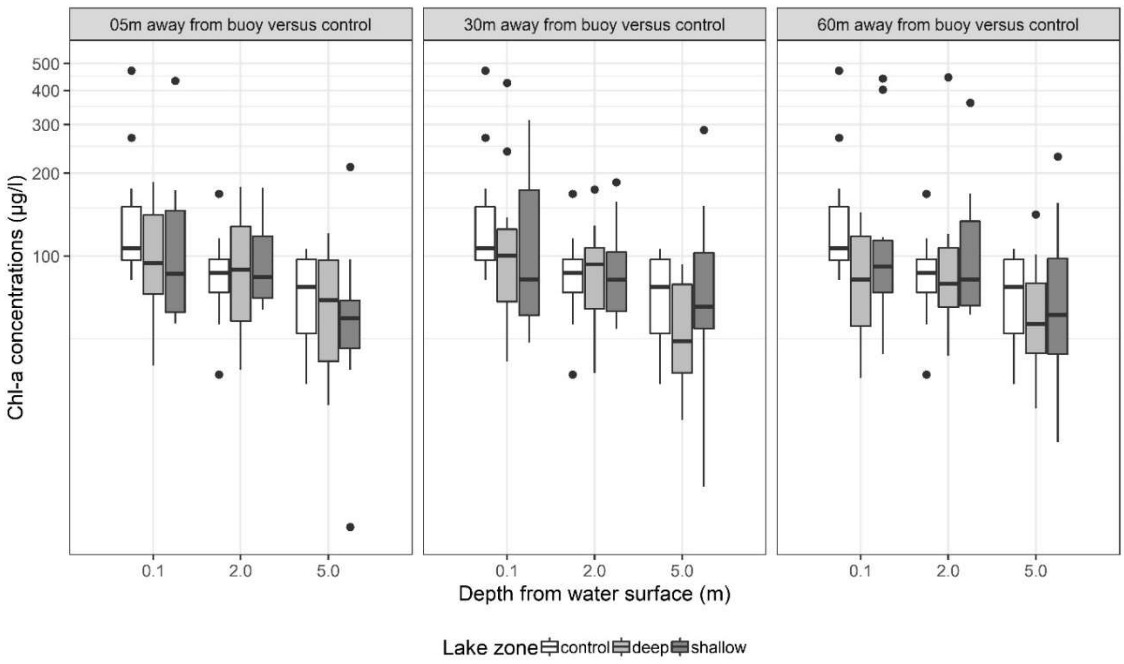

Figure 17 Chl-a concentrations at different locations compared to control over depths

The effect of the ultrasound on the vertical distribution of MC-LR (extra and intra-cellular) was statistically analysed by comparing surface toxin levels to those measured at 5 m depth. The mixed-linear model applied to the extracellular MC-LR concentrations did not show any statistically significant difference between surface toxin levels and those measured at a depth of 5 m; moreover, the toxin levels were largely similar to those measured at the control site (Figure 18). This largely indicates that the ultrasonic treatment did not lead to increased cell lysing nor to elevated toxin release. Our results concur with the findings of Li et al. (2014), who reported that sonicating at low frequency (20 kHz) and with low power does not promote toxin release. Note that other studies have reported that ultrasonic irradiations at low frequencies (< 40 kHz) can induce cell lysing and increase toxin concentrations in the water (Huang et al. 2020, Park et al. 2019). Moreover, our results did not indicate that the ultrasonic treatment had any significant role in degrading the toxin levels. This is to be expected given the low power used for the ultrasound devices (Park et al. 2019).

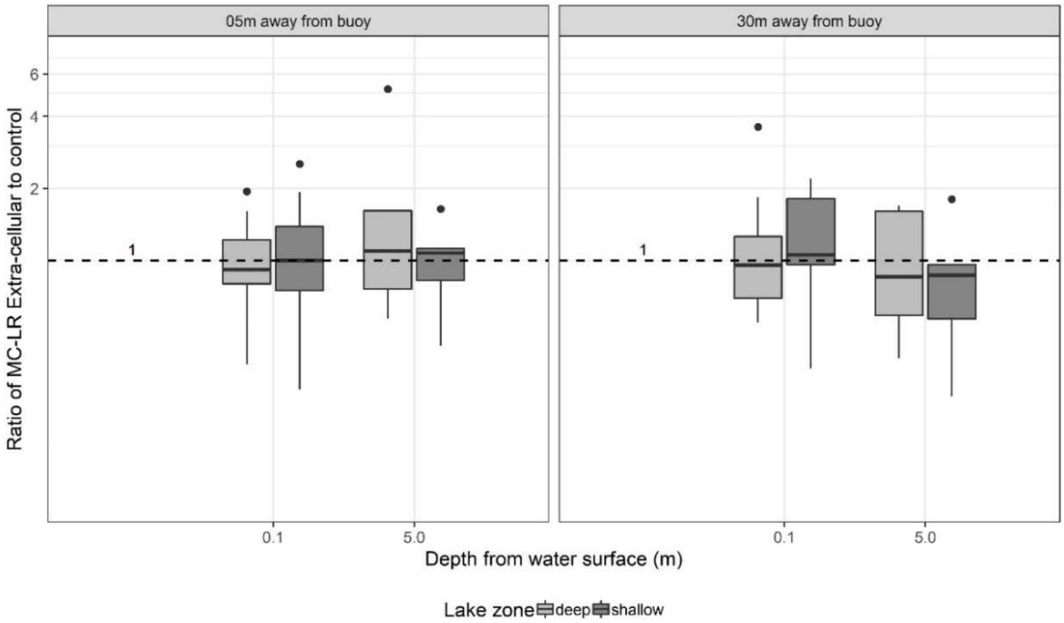

Figure 18. Variability of extracellular MC-LR levels by depth as compared to the control site: (a) shows the differences 5 m away from the buoy, (b) shows the differences 30 m away from the buoy

Regarding the intracellular MC-LR levels, we found that their natural variability at a given location was higher than their variability over depth. As such, surface levels were statistically similar to those measured at 5 m, with the exception of buoy 29B (5 m radial distance from the buoy) that had significantly higher surface intra-cellular MC-LR levels as compared to those measured at a depth of 5 m. Nevertheless, the median ratio of Chl-a levels to the intracellular MC-LR concentrations was lower (Wilcoxon rank sum test; p-value = 0.084) and close to the shallow ultrasonic buoy as compared to the control station (Figure 19). At a depth of 5 m (Figure 19), the sites in close proximity to the buoys maintained largely the same ratio of Chl-a to intracellular MC-LR, while the control site showed a significant drop in the ratio (Wilcoxon rank sum test; p-value = 0.03). These results suggest that the ultrasonic treatment may have increased the generation of intracellular toxins in the affected cells up to 5 m. Several studies have reported that the rate of MC-LR generation is amplified when the cyanobacteria are stressed (Brand et al. 2010, Kumar Rai et al. 2013, Zilliges et al. 2011).

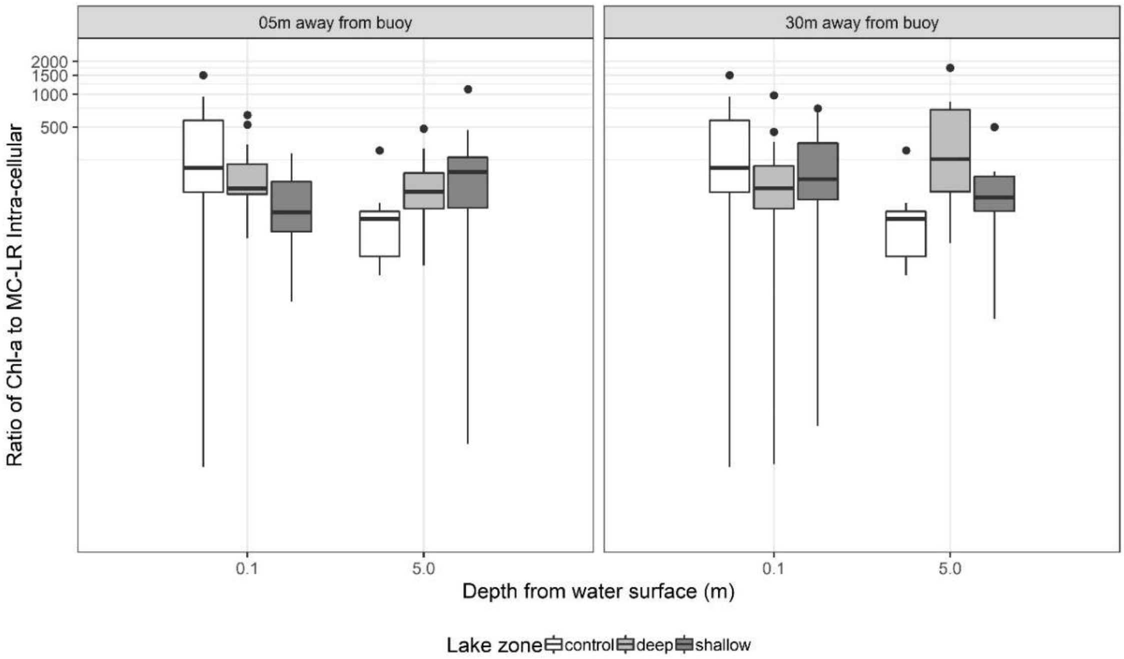

Figure 19. Variability of the ratio of Chl-a to intracellular MC-LR as a function of depth and distance to ultrasonic buoy

CHAPTER IV

CONCLUSION

This study is by far the most extensive and systematic assessment of the performance of ultrasonic treatment under real-time field conditions to date. It also reports the results from the largest freshwater system (220 million m^3) to have been fitted with one of the most extensive deployments of ultrasonic treatment systems (10 solar-powered ultrasonic buoys, each fitted with 4 transmitters) in the world. It is also the first attempt to assess concurrently how Chl-a concentrations, cyanotoxin levels, and ultrasonic wave frequencies and amplitudes changed over radial distances and depth, while concurrently comparing them to a control site on the same water body.

Our results showed that the ultrasonic transmitters were operational and emitting at frequencies ranging between 27 and 47 kHz. The sound emissions from the buoys was found to be dynamic over time and provides evidence that the operators were fine-tuning their transmitters based on data collected from the water quality sensors deployed in the lake and from satellite images. The ultrasonic recordings from the reservoir indicates that the influence of the deployed buoys was limited to a radial distance of 30 m and to a depth of 5 m. Moreover, analysing the collected water quality data from the lake showed no major improvements within the buoys’ regions of influence as compared to a control site on the same lake. Nevertheless, we observed a statistically significant difference in the vertical distribution of Chl-a levels over depth in the regions that were in close proximity to the emitting devices. In these regions, elevated algal levels were found up to 2 m in depth, which may suggest that the buoyancy of the cyanobacteria may have been altered by the emitted frequencies. Regarding toxin levels, the concentrations of extracellular MC-LR in the treated zones were found to be similar in magnitude to those in the control site and did not show a decline over depth. This highlights that the ultrasonic treatment did not promote cell lysing, toxin release, nor toxin breakdown. Yet, the results showed that intracellular toxin levels per unit of Chl-a tended to be higher near the ultrasonic transmitters as compared to the control site. This suggests that the emitted ultrasonic waves may have increased the stress levels on the cyanobacteria and thus accelerated their toxin transcription rates or promoted toxin-producing cells over their non-toxic forming cells (Brand et al. 2010, Kumar Rai et al. 2013, Zilliges et al. 2011).

We think that our results provide strong evidence that highlights the limitations that the current ultrasonic treatments suffer from regarding HAB management and control in the field. The inability of the ultrasonic devices to control HABs is probably due to many factors, including the short radial range over which the ultrasound can effectively influence the cyanobacterial cells as well as the inability of the deployed devices to emit high ultrasonic frequencies with enough high power. Higher power will require supplementing the buoys with electrical power to complement the power generated from the existing solar panels. Additionally, it is important to note that the ultrasonic devices were deployed in the reservoir in early summer when minor algal blooms started to be observed. As such, it is not possible to conclusively deduce how the HAB dynamics would have developed had the ultrasonic buoys been deployed earlier in the year. Similarly, the impact of having the buoys cover only half of the entire reservoir's surface area could not be properly quantified.

There is a need for additional field-based studies to better assess and understand the full potential of ultrasonication as an effective HAB control measure across different water systems. Additionally, more work is needed at the laboratory scale to resolve differences in proposed setup and reported performance. Future efforts need to focus on optimize the frequency(ies), power, and duration of the ultrasonic treatment and to assess if and how these change with the targeted cyanobacterial species. Additionally, there is a need to better understand the exact mechanism(s) (mechanical/chemical) by which the sonication inhibits HABs. In conclusion, we think that this work provides water establishments, who are considering the deployment of commercially available ultrasonic buoys on their HAB-affected freshwater systems as a new and environmentally safe mitigation measure, much needed guidance and a cautionary note about the limitations and risks of such an endeavour.

BIBLIOGRAPHY

Abraxis, E. (2020) Microcystins-ADDA SAES ELISA (Microtiter Plate) Streptavidin Amplified Enhanced Sensitivity Enzyme-Linked Immunosorbent Assay for the Congener-Independent* Determination of Microcystins and Nodularins in Water Samples, 124 Railroad Drive Warminster, PA 18974 USA.

Ahn, C.Y., Joung, S.H., Choi, A., Kim, H.S., Jang, K.Y. and Oh, H.M. (2007) Selective Control of Cyanobacteria in Eutrophic Pond by a Combined Device of Ultrasonication and Water Pumps. Environmental Technology 28(4), 371-379.

Betten, A., Braun, M., Fripertinger, H., Kerber, A., Kohnert, A. and Wassermann, A. (2006) Error-correcting linear codes: Classification by isometry and applications, Springer Science & Business Media.

Bilek, S.E. and Turantaş, F. (2013) Decontamination efficiency of high power ultrasound in the fruit and vegetable industry, a review. International Journal of Food Microbiology 166(1), 155-162.

Binding, C.E., Greenberg, T.A., McCullough, G., Watson, S.B. and Page, E. (2018) An analysis of satellite-derived chlorophyll and algal bloom indices on Lake Winnipeg. Journal of Great Lakes Research 44(3), 436-446.

Borkman, D.G. and Smayda, T.J. (2016) Coincident patterns of waste water suspended solids reduction, water transparency increase and chlorophyll decline in Narragansett Bay. Marine Pollution Bulletin 107(1), 161-169.

Brand, L.E., Pablo, J., Compton, A., Hammerschlag, N. and Mash, D.C. (2010) Cyanobacterial blooms and the occurrence of the neurotoxin, beta-N-methylamino-l-alanine (BMAA), in South Florida aquatic food webs. Harmful algae 9(6), 620-635.

Cameron, M., McMaster, L.D. and Britz, T.J. (2008) Electron microscopic analysis of dairy microbes inactivated by ultrasound. Ultrasonics sonochemistry 15(6), 960.

Chawla, I., Karthikeyan, L. and Mishra, A.K. (2020) A review of remote sensing applications for water security: Quantity, quality, and extremes. Journal of Hydrology 585, 124826.

Chen, G., Ding, X. and Zhou, W. (2020) Study on ultrasonic treatment for degradation of Microcystins (MCs). Ultrasonics Sonochemistry 63, 104900.

Christensson, P. (2006) Sample.

DataQ (2020) FFT (Fast Fourier Transform) Waveform Analysis.

Dehghani, M.H. (2016) Removal of cyanobacterial and algal cells from water by ultrasonic waves — A review. Journal of Molecular Liquids 222, 1109-1114.

Deutsch, E.S. and Alameddine, I. (2018) Hindcasting eutrophication and changes in temperature and storage volume in a semi-arid reservoir: a multi-decadal Landsat-based assessment. Environmental Monitoring and Assessment 191(1), 41.

Deutsch, E.S., Alameddine, I. and El-Fadel, M. (2018) Monitoring water quality in a hypereutrophic reservoir using Landsat ETM+ and OLI sensors: how transferable are the water quality algorithms? Environmental Monitoring and Assessment 190(3), 141.

Duan, Z., Tan, X. and Li, N. (2017) Ultrasonic selectivity on depressing photosynthesis of cyanobacteria and green algae probed by chlorophyll-a fluorescence transient. Water Science and Technology 76(8), 2085-2094.

Eaton, A. and Franson, M. (2005) American Water Works Association & Water Environment Federation 2005 Standard Methods for the Examination of Water and Wastewater. Washington, DC.

Eckersley, E. and Berger, B.W. (2018) An engineered polysaccharide lyase to combat harmful algal blooms. Biochemical Engineering Journal 132, 225-232.
ELARD (2011) Business Plan For Combating Pollution of The Qaraoun Lake, p. 475.
EPA (1978) Protective Noise Levels, National Service Center for Environmental Publications (NSCEP).
Fadel, A., Atoui, A., Lemaire, B.J., Vinçon-Leite, B. and Slim, K. (2015) Environmental factors associated with phytoplankton succession in a Mediterranean reservoir with a highly fluctuating water level. Environmental monitoring and assessment 187(10), 633.
Fadel, A., Faour, G. and Slim, K. (2016) Assessment of the trophic state and chlorophyll-a concentrations using Landsat OLI in Karaoun reservoir, Lebanon. Leban. Sci. J 17(2), 130-145.
Fadel, A. and Slim, K. (2018) The Litani River, Lebanon: An Assessment and Current Challenges. Shaban, A. and Hamzé, M. (eds), pp. 71-86, Springer International Publishing, Cham.
Fan, G., Lin, Q. and Chen, L. (2014) The Effect of Ultrasound on Microcystis sp. Morphological Characteristics at Different Ultrasonic Power. Nature Environment and Pollution Technology 13(1), 43-48.
Fang, C., Song, K., Li, L., Wen, Z., Liu, G., Du, J., Shang, Y. and Zhao, Y. (2018) Spatial variability and temporal dynamics of HABs in Northeast China. Ecological Indicators 90, 280-294.
Fang, S., Del Giudice, D., Scavia, D., Binding, C.E., Bridgeman, T.B., Chaffin, J.D., Evans, M.A., Guinness, J., Johengen, T.H. and Obenour, D.R. (2019) A space-time geostatistical model for probabilistic estimation of harmful algal bloom biomass and areal extent. Science of The Total Environment 695, 133776.
Fox, J. and Weisberg, S. (2011) An (R) Companion to Applied Regression, Sage, Thousand Oaks (CA).
Gobler, Christopher, Coyne, J., K., Dawson and Celia (2013) The Impact of Nutrients, Zooplankton, and Temperature on Growth of, and Toxin Production by, Cyanobacteria Blooms in the Upper Reaches of Chesapeake Bay, USEPA.
Gobler, C.J. (2020) Climate Change and Harmful Algal Blooms: Insights and perspective. Harmful Algae 91, 101731.
González, P.M. and Puntarulo, S. (2020) Possible role of seasonality and harmful algal blooms (HAB) on the oxidative and nitrosative metabolisms in hemocytes. Comparative Biochemistry and Physiology Part C: Toxicology & Pharmacology 232, 108744.
Greenly, J.M. and Tester, J.W. (2015) Ultrasonic cavitation for disruption of microalgae. Bioresource Technology 184, 276-279.
Hansen, C. (1995) FUNDAMENTALS OF ACOUSTICS, WHO.
Hao, H., Wu, M., Chen, Y., Tang, J. and Wu, Q. (2004a) Cavitation mechanism in cyanobacterial growth inhibition by ultrasonic irradiation. Colloids and Surfaces B: Biointerfaces 33(3), 151-156.
Hao, H., Wu, M., Chen, Y., Tang, J. and Wu, Q. (2004b) Cyanobacterial Bloom Control by Ultrasonic Irradiation at 20 kHz and 1.7 MHz. Journal of Environmental Science and Health, Part A 39(6), 1435-1446.
Hass, J. (2018) An Acoustics Primer, Indiana University.
Heng, L., Jun, N., Wen-jie, H. and Guibai, L. (2009) Algae removal by ultrasonic irradiation–coagulation. Desalination 239(1), 191-197.

Huang, J., Zhang, Y., Huang, Q. and Gao, J. (2018) When and where to reduce nutrient for controlling harmful algal blooms in large eutrophic lake Chaohu, China? Ecological Indicators 89, 808-817.
Huang, Y.-R., Li, H.-Z., Wei, X.-M., Wang, D.-H., Liu, Y.-T. and Li, L. (2020) The effect of low frequency ultrasonic treatment on the release of extracellular organic matter of Microcystis aeruginosa. Chemical Engineering Journal 383, 123141.
Hydrophones, A. (2020) AS-1 HYDROPHONE.
Inman, D. (2004) Ultrasonic treatment of algae, Cranfield University, School of Water Sciences.
Iwinski, K.J., Rodgers, J.H., Kinley, C.M., Hendrikse, M., Calomeni, A.J., McQueen, A.D., Geer, T.D., Liang, J., Friesen, V. and Haakensen, M. (2017) Influence of CuSO4 and chelated copper algaecide exposures on biodegradation of microcystin-LR. Chemosphere 174, 538-544.
Jachlewski, S., Botes, M. and Cloete, T.E. (2013) The effect of ultrasound at 256 KHz on Microcystis aeruginosa, with and without gas vacuoles. Water S.A. 39(1), 171-174.
Jančula, D. and Maršálek, B. (2011) Critical review of actually available chemical compounds for prevention and management of cyanobacterial blooms. Chemosphere 85(9), 1415-1422.
Joyce, E., Phull, S.S., Lorimer, J.P. and Mason, T.J. (2003) The development and evaluation of ultrasound for the treatment of bacterial suspensions. A study of frequency, power and sonication time on cultured Bacillus species. Ultrasonics sonochemistry 10(6), 315.
Joyce, E.M., Wu, X. and Mason, T.J. (2010) Effect of ultrasonic frequency and power on algae suspensions. Journal of Environmental Science and Health, Part A 45(7), 863-866.
Jurdi, M., Korfali, S.I., Karahagopian, Y. and Davies, B.E. (2002) Evaluation of water quality of the Qaraaoun Reservoir, Lebanon: Suitability for multipurpose usage. Environmental Monitoring and Assessment 77(1), 11-30.
Kardinaal, E., De Haan, M. and Ruiter, H. (2008) Maatregelen ter voorkoming blauwalgen werken onvoldoende. H2O 41(7), 4.
Kherad-pajouh, S. and Renaud, O. (2015) A general permutation approach for analyzing repeated measures ANOVA and mixed-model designs. Statistical Papers 56(4), 947-967.
Kinley, C.M., Iwinski, K.J., Hendrikse, M., Geer, T.D. and Rodgers, J.H. (2017) Cell density dependence of Microcystis aeruginosa responses to copper algaecide concentrations: Implications for microcystin-LR release. Ecotoxicology and Environmental Safety 145, 591-596.
Koda, S., Miyamoto, M., Toma, M., Matsuoka, T. and Maebayashi, M. (2009) Inactivation of Escherichia coli and Streptococcus mutans by ultrasound at 500kHz. Ultrasonics sonochemistry 16(5), 655.
Kong, Y., Peng, Y., Zhang, Z., Zhang, M., Zhou, Y. and Duan, Z. (2019) Removal of Microcystis aeruginosa by ultrasound: Inactivation mechanism and release of algal organic matter. Ultrasonics Sonochemistry 56, 447-457.
Kotopoulis, S., Schommartz, A. and Postema, M. (2009) Sonic cracking of blue-green algae. Applied Acoustics 70(10), 1306-1312.
Kumar Rai, A., Pearson, L.A. and Kumar, A. (2013) Stress Biology of Cyanobacteria: Molecular Mechanisms to Cellular Responses. Srivastava, A.K., Rai, A.N. and Neilan, B.A. (eds), pp. 341-347, CRC Press, Boca Raton, FL.

Kurokawa, M., King, P.M., Wu, X., Joyce, E.M., Mason, T.J. and Yamamoto, K. (2016) Effect of sonication frequency on the disruption of algae. Ultrasonics Sonochemistry 31, 157-162.
Laird, N.M. and Ware, J.H. (1982) Random-Effects Models for Longitudinal Data.
LaLiberte, G. and Haber, E. (2014) Literature Review of the Effects of Ultrasonic Waves on Cyanobacteria, Other Aquatic Organisms, and Water Quality, Bureau of Science Services, Madison WI.
Larson, J.H., Richardson, W.B., Evans, M.A., Schaeffer, J., Wynne, T., Bartsch, M., Bartsch, L., Nelson, J. and Vallazza, J. (2016) Measuring spatial variation in secondary production and food quality using a common consumer approach in Lake Erie. Ecological Applications 26(3), 873-885.
Lee, T.J., Nakano, K. and Matsumara, M. (2001) Ultrasonic Irradiation for Blue-Green Algae Bloom Control. Environmental Technology 22(4), 383-390.
Lee, T.J., Nakano, K. and Matsumura, M. (2002) A novel strategy for cyanobacterial bloom control by ultrasonic irradiation. Water science and technology : a journal of the International Association on Water Pollution Research 46(6-7), 207-215.
Lee, Z., Shang, S., Hu, C., Du, K., Weidemann, A., Hou, W., Lin, J. and Lin, G. (2015) Secchi disk depth: A new theory and mechanistic model for underwater visibility. Remote Sensing of Environment 169, 139-149.
Lei, S., Xu, J., Li, Y., Du, C., Liu, G., Zheng, Z., Xu, Y., Lyu, H., Mu, M., Miao, S., Zeng, S., Xu, J. and Li, L. (2020) An approach for retrieval of horizontal and vertical distribution of total suspended matter concentration from GOCI data over Lake Hongze. Science of The Total Environment 700, 134524.
Leighton, T.G. (2007) What is ultrasound? Progress in Biophysics and Molecular Biology 93(1), 3-83.
Lenth, R.V. (2016) Least-Squares Means: The (R) Package (lsmeans).
LGSONIC (2020a) Algae and Biofouling Control Products.
LGSONIC (2020b) Control and Monitor Algae with the MPC-Buoy.
Li, J., Hu, J., Cao, L. and Yuan, Y. (2020) Growth, physiological responses and microcystin-production/-release dynamics of Microcystis aeruginosa exposed to various luteolin doses. Ecotoxicology and Environmental Safety 196, 110540.
Li, J., Long, H., Song, C., Wu, W., Yeabah, T.O. and Qiu, Y. (2014) Study on the removal of algae from lake water and its attendant water quality changes using ultrasound. Desalination and Water Treatment 52(25-27), 4762-4771.
Li, Y., Shi, X., Zhang, Z. and Peng, Y. (2019) Enhanced coagulation by high-frequency ultrasound in Microcystis aeruginosa-laden water: Strategies and mechanisms. Ultrasonics Sonochemistry 55, 232-242.
Lihong, D.Y.P.Y.Y. and Wei, Q.X.L.Y.W. (2009) Parameters optimization of ultrasound algae removal technology and bloom removal study in Taihu Lake [J]. Journal of Southeast University (Natural Science Edition) 2.
Liu, C., Wang, J., Cao, Z., Chen, W. and Bi, H. (2016) Variation of dissolved organic nitrogen concentration during the ultrasonic pretreatment to Microcystis aeruginosa. Ultrasonics Sonochemistry 29, 236-243.
Lürling, M., Meng, D. and Faassen, E. (2014) Effects of hydrogen peroxide and ultrasound on biomass reduction and toxin release in the cyanobacterium, Microcystis aeruginosa. Toxins 6, 3260–3280.
Lürling, M. and Tolman, Y. (2014) Beating the blues: Is there any music in fighting cyanobacteria with ultrasound? Water Research 66, 361-373.

Lurling, M., Waajen, G. and de Senerpont Domis, L. (2016) Evaluation of several end-of-pipe measures proposed to control cyanobacteria. Aquatic ecology 50(3), 499-519.
Ma, B., Chen, Y., Hao, H., Wu, M., Wang, B., Lv, H. and Zhang, G. (2005) Influence of ultrasonic field on microcystins produced by bloom-forming algae. Colloids and Surfaces B: Biointerfaces 41(2), 197-201.
MicroPyramid (2017) Understanding Audio Quality: Bit Rate, Sample Rate.
Miller, T.R., Beversdorf, L., Chaston, S.D. and McMahon, K.D. (2013) Spatiotemporal molecular analysis of cyanobacteria blooms reveals Microcystis-Aphanizomenon interactions. PloS one 8(9), e74933.
Moore, S.K., Cline, M.R., Blair, K., Klinger, T., Varney, A. and Norman, K. (2019) An index of fisheries closures due to harmful algal blooms and a framework for identifying vulnerable fishing communities on the U.S. West Coast. Marine Policy, 103543.
Nishijima, W., Umehara, A., Sekito, S., Wang, F., Okuda, T. and Nakai, S. (2018) Determination and distribution of region-specific background Secchi depth based on long-term monitoring data in the Seto Inland Sea, Japan. Ecological Indicators 84, 583-589.
NPS (2018) Understanding Sound, Natural Park Service
U.S. Department of the Interior.
O'Brien, W.D. (2007) Ultrasound–biophysics mechanisms. Progress in Biophysics and Molecular Biology 93(1), 212-255.
Ott, W.R. (1995) Environmental statistics and data analysis.
Park, C.B., Baik, S., Kim, S., Choi, J.W., Lee, S.H. and Kim, Y.J. (2017a) The use of ultrasonic frequencies to control the bloom formation, regrowth, and eco-toxicity in Microcystis aeruginosa. International Journal of Environmental Science and Technology 14(5), 923-932.
Park, J., Church, J., Son, Y., Kim, K.-T. and Lee, W.H. (2017b) Recent advances in ultrasonic treatment: Challenges and field applications for controlling harmful algal blooms (HABs). Ultrasonics Sonochemistry 38, 326-334.
Park, J., Son, Y. and Lee, W.H. (2019) Variation of efficiencies and limits of ultrasonication for practical algal bloom control in fields. Ultrasonics Sonochemistry 55, 8-17.
Patel, N., Ruparelia, J. and Barve, J. (2020) Prediction of total suspended solids present in effluent of primary clarifier of industrial common effluent treatment plant: Mechanistic and fuzzy approach. Journal of Water Process Engineering 34, 101146.
Peng, Y., Zhang, Z., Kong, Y., Li, Y., Zhou, Y., Shi, X. and Shi, X. (2020) Effects of ultrasound on Microcystis aeruginosa cell destruction and release of intracellular organic matter. Ultrasonics Sonochemistry 63, 104909.
Pike, J. (1998) Underwater Acoustics.
Pinheiro, J., Bates, D., DebRoy, S., Sarkar, D. and Team, R.C. (2020) *nlme: Linear and Nonlinear Mixed Effects Models*.
Purcell, D., Parsons, S.A. and Jefferson, B. (2013a) The influence of ultrasound frequency and power, on the algal species Microcystis aeruginosa, Aphanizomenon flos-aquae, Scenedesmus subspicatus and Melosira sp. Environmental Technology 34(17), 2477-2490.
Purcell, D., Parsons, S.A., Jefferson, B., Holden, S., Campbell, A., Wallen, A., Chipps, M., Holden, B. and Ellingham, A. (2013b) Experiences of algal bloom control using green solutions barley straw and ultrasound, an industry perspective. Water and Environment Journal 27(2), 148-156.

Qin, B., Paerl, H.W., Brookes, J.D., Liu, J., Jeppesen, E., Zhu, G., Zhang, Y., Xu, H., Shi, K. and Deng, J. (2019) Why Lake Taihu continues to be plagued with cyanobacterial blooms through 10 years (2007–2017) efforts. Science Bulletin 64(6), 354-356.
Qin, Q. and Shen, J. (2019) Physical transport processes affect the origins of harmful algal blooms in estuaries. Harmful Algae 84, 210-221.
R Core Team (2019) R: A language and environment for statistical computing, R Foundation for Statistical Computing, Vienna, Austria.
Rajasekhar, P., Fan, L., Nguyen, T. and Roddick, F.A. (2012a) Impact of sonication at 20 kHz on Microcystis aeruginosa, Anabaena circinalis and Chlorella sp. Water Research 46(5), 1473-1481.
Rajasekhar, P., Fan, L., Nguyen, T. and Roddick, F.A. (2012b) A review of the use of sonication to control cyanobacterial blooms. Water Research 46(14), 4319-4329.
Rarrek, A., Rehfeldt, S. and Klein, H. (2018) Evaluation of CO2 gas supply of large open algae ponds. Chemical Engineering Science 187, 432-443.
rdrr (2019a) meanspec : Mean frequency spectrum of a time wave.
rdrr (2019b) rms : Root Mean Square.
Rice, E.W., Baird, R.B., Eaton, A.D. and Clesceri, L.S. (2012) Standard methods for the examination of water and wastewater, American Public Health Association Washington, DC.
Rijal Leblad, B., Amnhir, R., Reqia, S., Sitel, F., Daoudi, M., Marhraoui, M., Ouelad Abdellah, M.K., Veron, B., Er-Raioui, H. and Laabir, M. (2020) Seasonal variations of phytoplankton assemblages in relation to environmental factors in Mediterranean coastal waters of Morocco, a focus on HABs species. Harmful Algae 96, 101819.
Rinta-Kanto, J.M., Konopko, E.A., DeBruyn, J.M., Bourbonniere, R.A., Boyer, G.L. and Wilhelm, S.W. (2009) Lake Erie Microcystis: Relationship between microcystin production, dynamics of genotypes and environmental parameters in a large lake. Harmful Algae 8(5), 665-673.
Rodriguez-Molares, A., Dickson, S., Hobson, P., Howard, C., Zander, A. and Burch, M. (2014) Quantification of the ultrasound induced sedimentation of Microcystis aeruginosa. Ultrasonics Sonochemistry 21(4), 1299-1304.
Rolle Longley, K., Huang, W., Clark, C. and Johnson, E. (2019) Effects of nutrient load from St. Jones River on water quality and eutrophication in Lake George, Florida. Limnologica 77, 125687.
Sadeghian, A., Chapra, S.C., Hudson, J., Wheater, H. and Lindenschmidt, K.-E. (2018) Improving in-lake water quality modeling using variable chlorophyll a/algal biomass ratios. Environmental Modelling & Software 101, 73-85.
Sakai, H., Oguma, K., Katayama, H. and Ohgaki, S. (2007) Effects of low or medium-pressure UV irradiation on the release of intracellular microcystin. Water Research 41(15), 3458-3464.
Schneider, O.D., Weinrich, L.A. and Brezinski, S. (2015) Ultrasonic Treatment of Algae in a New Jersey Reservoir. Journal - American Water Works Association 107(10), E533-E542.
Şengül, A.B., Ersan, G. and Tüfekçi, N. (2018) Removal of intra- and extracellular microcystin by submerged ultrafiltration (UF) membrane combined with coagulation/flocculation and powdered activated carbon (PAC) adsorption. Journal of Hazardous Materials 343, 29-35.

Sinang, S.C., Reichwaldt, E.S. and Ghadouani, A. (2013) Spatial and temporal variability in the relationship between cyanobacterial biomass and microcystins. Environmental Monitoring and Assessment 185(8), 6379-6395.
Singh, S. (2019) Climate Change and Agricultural Ecosystems. Choudhary, K.K., Kumar, A. and Singh, A.K. (eds), pp. 249-263, Woodhead Publishing.
Song, W., de la Cruz, A.A., Rein, K. and O'Shea, K.E. (2006) Ultrasonically Induced Degradation of Microcystin-LR and -RR: Identification of Products, Effect of pH, Formation and Destruction of Peroxides. Environmental Science & Technology 40(12), 3941-3946.
Song, W., Teshiba, T., Rein, K. and O'Shea, K.E. (2005) Ultrasonically Induced Degradation and Detoxification of Microcystin-LR (Cyanobacterial Toxin). Environmental Science & Technology 39(16), 6300-6305.
Su, X., Steinman, A.D., Tang, X., Xue, Q., Zhao, Y. and Xie, L. (2017) Response of bacterial communities to cyanobacterial harmful algal blooms in Lake Taihu, China. Harmful Algae 68, 168-177.
Sueur, J., Aubin, T. and Simonis, C. (2008) SEEWAVE, A FREE MODULAR TOOL FOR SOUND ANALYSIS AND SYNTHESIS. Bioacoustics 18(2), 213-226.
Sun, R., Sun, P., Zhang, J., Esquivel-Elizondo, S. and Wu, Y. (2018) Microorganisms-based methods for harmful algal blooms control: A review. Bioresource Technology 248, 12-20.
Tan, X., Shu, X., Guo, J., Parajuli, K., Zhang, X. and Duan, Z. (2018a) Effects of Low-Frequency Ultrasound on <i>Microcystis aeruginosa</i> from Cell Inactivation to Disruption. Bulletin of Environmental Contamination and Toxicology 101(1), 117-123.
Tan, X., Zhang, D., Parajuli, K., Upadhyay, S., Jiang, Y. and Duan, Z. (2018b) Comparison of Four Quantitative Techniques for Monitoring Microalgae Disruption by Low-Frequency Ultrasound and Acoustic Energy Efficiency. Environmental Science & Technology 52(5), 3295-3303.
Tang, J.W., Wu, Q.Y., Hao, H.W., Chen, Y. and Wu, M. (2004) Effect of 1.7 MHz ultrasound on a gas-vacuolate cyanobacterium and a gas-vacuole negative cyanobacterium. Colloids and Surfaces B: Biointerfaces 36(2), 115-121.
Techer, D. and Banas, D. (2018) Contrasted effects of an anti-cyanobacterial ultrasound device on the non-target freshwater invertebrate species Gammarus roeseli. Environmental Science and Pollution Research 25(2), 1998-2004.
Tekile, A., Kim, I. and Lee, J.-Y. (2017) 200 kHz Sonication of Mixed-Algae Suspension from a Eutrophic Lake: The Effect on the Caution vs. Outbreak Bloom Alert Levels. Water 9(12), 915.
Tsai, K.-P. (2015) Effects of two copper compounds on Microcystis aeruginosa cell density, membrane integrity, and microcystin release. Ecotoxicology and Environmental Safety 120, 428-435.
USAID (2005) Litani water quality management project: rapid review report., Development Alternatives, Inc. (DAI).
Wang, M., Strokal, M., Burek, P., Kroeze, C., Ma, L. and Janssen, A.B.G. (2019) Excess nutrient loads to Lake Taihu: Opportunities for nutrient reduction. Science of The Total Environment 664, 865-873.
Weirich, C.A. and Miller, T.R. (2014) Freshwater Harmful Algal Blooms: Toxins and Children's Health. Current Problems in Pediatric and Adolescent Health Care 44(1), 2-24.

Wells, M.L., Karlson, B., Wulff, A., Kudela, R., Trick, C., Asnaghi, V., Berdalet, E., Cochlan, W., Davidson, K., De Rijcke, M., Dutkiewicz, S., Hallegraeff, G., Flynn, K.J., Legrand, C., Paerl, H., Silke, J., Suikkanen, S., Thompson, P. and Trainer, V.L. (2020) Future HAB science: Directions and challenges in a changing climate. Harmful Algae 91, 101632.
WHO (2003) Cyanobacterial toxins: Microcystin-LR in Drinking-water, World Health Organization, Geneva, 1998.
Wolf, D., Georgic, W. and Klaiber, H.A. (2017) Reeling in the damages: Harmful algal blooms' impact on Lake Erie's recreational fishing industry. Journal of Environmental Management 199, 148-157.
Wu, X., Joyce, E.M. and Mason, T.J. (2011) The effects of ultrasound on cyanobacteria. Harmful Algae 10(6), 738-743.
Wu, X., Joyce, E.M. and Mason, T.J. (2012) Evaluation of the mechanisms of the effect of ultrasound on Microcystis aeruginosa at different ultrasonic frequencies. Water Research 46(9), 2851-2858.
Wu, X., Liu, J. and Zhu, J.-J. (2019) Sono-Fenton hybrid process on the inactivation of Microcystis aeruginosa: Extracellular and intracellular oxidation. Ultrasonics Sonochemistry 53, 68-76.
Xiang, L., Li, Y.-W., Liu, B.-L., Zhao, H.-M., Li, H., Cai, Q.-Y., Mo, C.-H., Wong, M.-H. and Li, Q.X. (2019) High ecological and human health risks from microcystins in vegetable fields in southern China. Environment International 133, 105142.
Yacobi, Y.Z., Köhler, J., Leunert, F. and Gitelson, A. (2015) Phycocyanin-specific absorption coefficient: Eliminating the effect of chlorophylls absorption. Limnology and Oceanography: Methods 13(4), 157-168.
Yamamoto, K., King, P.M., Wu, X., Mason, T.J. and Joyce, E.M. (2015) Effect of ultrasonic frequency and power on the disruption of algal cells. Ultrasonics Sonochemistry 24, 165-171.
Yamamoto, Y. and Shiah, F.-K. (2015) Effect of sonication on live and fixed cells of Microcystis aeruginosa. Plankton & Benthos Research 10(3), 163.
Yan, Y., Bao, Z. and Shao, J. (2018) Phycocyanin concentration retrieval in inland waters: A comparative review of the remote sensing techniques and algorithms. Journal of Great Lakes Research 44(4), 748-755.
Yu, G., Zhao, C., Liu, B., Li, Q. and Gao, H. (2013) Removal of algae from raw water by ultrasonic irradiation and flocculation: A pilot scale experiment. Journal of Environmental Biology 34(2 suppl), 331-335.
Yu, J., Fan, C., Zhong, J., Zhang, Y., Wang, C. and Zhang, L. (2016) Evaluation of in situ simulated dredging to reduce internal nitrogen flux across the sediment-water interface in Lake Taihu, China. Environmental Pollution 214, 866-877.
Zeng, S., Yuan, X., Shi, X. and Qiu, Y. (2010) Effect of inoculum/substrate ratio on methane yield and orthophosphate release from anaerobic digestion of Microcystis spp. Journal of Hazardous Materials 178(1), 89-93.
Zhang, G., Zhang, P., Liu, H. and Wang, B. (2006) Ultrasonic damages on cyanobacterial photosynthesis. Ultrasonics Sonochemistry 13(6), 501-505.
Zhang, H., Meng, G., Mao, F., Li, W., He, Y., Gin, K.Y.-H. and Ong, C.N. (2019) Use of an integrated metabolomics platform for mechanistic investigations of three commonly used algaecides on cyanobacterium, Microcystis aeruginosa. Journal of Hazardous Materials 367, 120-127.

Zhong, W., Zhang, Z., Luo, Y., Qiao, W., Xiao, M. and Zhang, M. (2012) Biogas productivity by co-digesting Taihu blue algae with corn straw as an external carbon source. Bioresource Technology 114, 281-286.
Zhou, S., Shao, Y., Gao, N., Deng, Y., Qiao, J., Ou, H. and Deng, J. (2013) Effects of different algaecides on the photosynthetic capacity, cell integrity and microcystin-LR release of Microcystis aeruginosa. Science of The Total Environment 463-464, 111-119.
Zhou, T., Cao, H., Zheng, J., Teng, F., Wang, X., Lou, K., Zhang, X. and Tao, Y. (2020) Suppression of water-bloom cyanobacterium Microcystis aeruginosa by algaecide hydrogen peroxide maximized through programmed cell death. Journal of Hazardous Materials 393, 122394.
Zilliges, Y., Kehr, J.-C., Meissner, S., Ishida, K., Mikkat, S., Hagemann, M., Kaplan, A., Boerner, T. and Dittmann, E. (2011) The cyanobacterial hepatotoxin microcystin binds to proteins and increases the fitness of Microcystis under oxidative stress conditions. PloS one 6(3), e17615.
ZOOM (2020) The ZOOM H5.
Zou, W., Zhu, G., Cai, Y., Vilmi, A., Xu, H., Zhu, M., Gong, Z., Zhang, Y. and Qin, B. (2020) Relationships between nutrient, chlorophyll a and Secchi depth in lakes of the Chinese Eastern Plains ecoregion: Implications for eutrophication management. Journal of Environmental Management 260, 109923.